Rapport final du 15.12.2014

Thermochromic coatings for overheating protection of solar collectors – temperature matching and triggering

(Thermochromie III)

Auteurs:

Dr. Antonio Paone, EPFL/LESO-PB, antonio.paone@epfl.ch
Anna Krammer, EPFL/LESO-PB, anna.krammer@epfl.ch
Raman Kukreja, EPFL/LESO-PB, raman.kukreja@epfl.ch
Olivia Bouvard, EPFL/LESO-PB, olivia.bouvard@epfl.ch
Mario Geiger, EPFL/LESO-PB, mario.geiger@epfl.ch
Dr. Andreas Schüler, EPFL/LESO-PB, andreas.schueler@epfl.ch

Le ou les auteurs sont seuls responsables du contenu et des conclusions de ce rapport.

Highlights of this Report

- **Temperature of the thermochromic transition raised** from 68°C to approx. 85°C by novel kind of doping

- Mechanism of **triggering** the transition of thermochromic or thermotropic collector glazing by emissivity switch of the thermochromic selective coating

- Precise **determination of the optical constants** of the thermochromic material in the states below and above the transition temperature

Summary

Overheating and the resulting stagnation of solar thermal collectors is a common problem even in central European latitudes. The high temperatures occurring during stagnation lead to water evaporation, glycol degradation and stresses in the collector with increasing vapour pressure. Special precautions are necessary to release this pressure; only mechanical solutions exist nowadays. Additionally, the elevated temperatures lead to degradation of the materials that compose the collector, such as sealing, thermal insulation and the selective absorber coating. The goal of this project is to find a new way of protecting solar thermal systems without any mechanical device (e.g. for shading or for pressure release). Novel thermochromic coatings are developed, which exhibit a change in optical properties at a critical temperature T_c.

Undoped, tungsten, aluminium, D1 and D2 doped samples of inorganic coatings showing thermochromic switching behaviour are produced by magnetron sputtering. A dynamical switching of the thermal emittance ε can be achieved by thermochromic transition metal oxides.

The effects of doping thermochromic oxide films by tungsten, aluminium, D1 and D2 have been studied in great detail. The structural and optical properties of these films have been characterized by methods such as X-ray diffraction (XRD) for phase identification, Rutherford backscattering spectrometry (RBS) and X-ray photoelectron spectrometry (XPS) for quantitatively determining the doping concentration and Energy-dispersive X-ray spectroscopy (EDX) for determining the chemical composition.

The performance of a solar collector with an absorber based on a thermochromic film has been simulated in order to determine the stagnation temperature and the produced energy as a function of the thermochromic transition temperature.

In parallel, the possibility of using the switch in emissivity of the absorber coating in order to trigger the transition of a thermochromic or thermotropic coating on the glazing of the solar collector has been studied. In a first step, an analytical approach yielded the required transition temperature of such a switching glazing. Subsequently, the availability of thermotropic glass and other kind of smart glass have been studied. Samples of identified commercial products were characterised to know their optical properties and define if they would be suitable for our application.

The fascinating optical properties of these switchable films elucidate the way towards novel "intelligent" thermal solar collector materials.

Project Goals

The main objective of this project is to limit the stagnation temperature of solar collectors to a value below the boiling point of the heat transfer liquid without degrading the optical performance of the selective coating during normal operation.

Advantages:

- Evaporation of the heat transfer liquid due to overheating will be avoided and the hydraulic system can be simplified.

- The lifetime of the collector materials used for thermal insulation, the joints and the selective coating itself will increase.

- The glycol component of the heat transfer liquid will be protected from degradation.

We target an optical switching behaviour for selective coatings. This change in the optical properties will occur at a critical temperature T_c. For solar thermal collectors a suitable transition temperature would be approximately 95°C. The temperature range under the critical temperature defines the standard working condition for the collector. In this range, the solar absorptance α should correspond to 95% and the thermal emittance ε to maximum 5%. The solar collector suffers overheating connected problems and resulting stagnation above the transition temperature. In this temperature range, the input of solar energy has to be reduced. Therefore, the solar absorptance α should correspond to 35% and the thermal emittance ε to above 40%.

Since we have already shown that the durability of organic thermochromic paints is not high enough for the considered application [Huo08], we focus on inorganic materials in this project: thermochromic transition metal oxides.

Project Goals 2014

A. Effect of doping - Film characterization of doped and undoped individual layers

- Structural investigation by X-ray diffraction (XRD) of undoped and doped by tungsten, aluminium, D1 and D2 thermochromic films.

- Chemical investigation by Rutherford backscattering spectrometry (RBS) of undoped and doped by tungsten and aluminium thermochromic films.

- Chemical investigation by Energy-dispersive X-ray spectroscopy (EDX) and X-ray photoelectron spectrometry (XPS) of undoped and doped by D1 and D2 thermochromic films.

- Determination of the optical properties of undoped and doped by tungsten thermochromic transition metal oxide films for both the low and the high temperature state inferred by spectroscopic ellipsometry in the VIS-MIR spectral range.

B. Computer simulations of solar thermal energy systems

- Simulation of emittance switching with thickness increasing for thermochromic transition metal oxide films.

- Simulation of reflectance switching of an optimized multilayer deposed on an aluminium substrate and composed by a thermochromic film and an antireflection coating.

- Calculations for the estimation of the stagnation temperature of a thermal solar collector adopting a thermochromic coating.

- Determination of the produced energy as a function of the thermochromic transition temperature.

C. Thermal coupling of coating on absorber sheet and glazing

- Modelling heat transfer between solar absorber and specific glazing. Determination of suitable switching temperature.

D. Switchable glazing: Market analysis and characterisation

- Market analysis on dynamic glazing. Identification of manufacturers and distributors. Study of the availability of thermotropic glazing.

- Characterisation of existing products: thermotropic glass and alternative product, e.g. switchable mirror.

Approach

A. Effect of doping - Film characterization of doped and undoped individual layers

At a critical temperature T_c, thermochromic metal oxide films undergo a reversible phase transition from a metallic to a semiconducting state, resulting in a sudden change in thermal emissivity and in a resistance change of typically three orders of magnitude.

Undoped coatings switch from semiconducting to metallic state at critical temperatures around 68°C.

The transition temperature of these doped films can be altered by suitable doping. Doped thermochromic metal oxide films are deposited by reactive magnetron co-sputtering of metallic targets in argon/oxygen atmosphere.

In order to verify whether the desired thermochromic crystalline phase is obtained, structural analyses of the deposited films are performed by X-ray diffraction (XRD).

Chemical analyses of the deposited films are performed by Rutherford backscattering spectrometry (RBS) and X-ray photoelectron spectrometry (XPS). These techniques allow us to determine precisely the respective atom concentrations of the elements present in the film. Chemical analyses of the deposited films are performed also by Energy-dispersive X-ray spectroscopy (EDX). The EDX technique allows us to qualitative estimate the respective atom concentrations of the elements present in the film.

B. Computer simulations of solar thermal energy systems

The optical properties of thermochromic transition metal oxide films for both the low and the high temperature state are inferred by spectroscopic ellipsometry in the VIS-MIR spectral range. These data can be used as basis for computer simulations predicting the reflectance, the solar absorptance and the thermal emittance on an aluminium substrate. The stagnation temperature of a collector adopting as absorber a thermochromic film doped by tungsten deposited on an aluminium substrate is determined using appropriate physical models [Bal08, Vries98, Zon03].

Using the solar absorptance and the thermal emittance determined for our thermochromic solar absorber coatings, the produced energy as a function of the thermochromic transition temperature was determined by PolySun simulations.

C. Thermal coupling of coating on absorber sheet and glazing

In order to further increase the switch in absorptance of the solar collector, it was investigated whether the emittance switch of the thermochromic absorber could trigger the transition of a thermotropic or thermochromic coating on the solar collector glazing.

The heat transfer from the absorber sheet to the glazing is simulated by a finite element approach or directly calculated by an analytical nodal model based on the equivalent electric circuit.

D. Switchable glazing : Market analysis and characterisation

In section C the thermal coupling between the absorber sheet and the glazing is studied. With its change in emissivity, the absorber could trigger the transition of a dynamic glazing such as a thermotropic or thermochromic one.

A study of the commercially available products is performed. Different sources are investigated: market studies and forecasts on smart glass, scientific literature on tested products, companies identified from patents and internet search.

Main manufacturers are stated and samples of identified products are obtained. Characterisations are performed in order to measure transmittance and reflectance in both states. The considered products exhibit a transition of their state implying a change of their optical properties. The aim here is to determine whether the current available products would meet our needs.

Description of Work and Results

A.   Effect of doping - Film characterization of doped individual layers

A.1.   Electrical properties of thermochromic films – tungsten doping

The MF (Medium Frequency) power applied to the principal target was kept constant while the RF-power applied to the doping target, tungsten, was varied. The transition temperature is reduced proportionally with increasing power on the tungsten target.
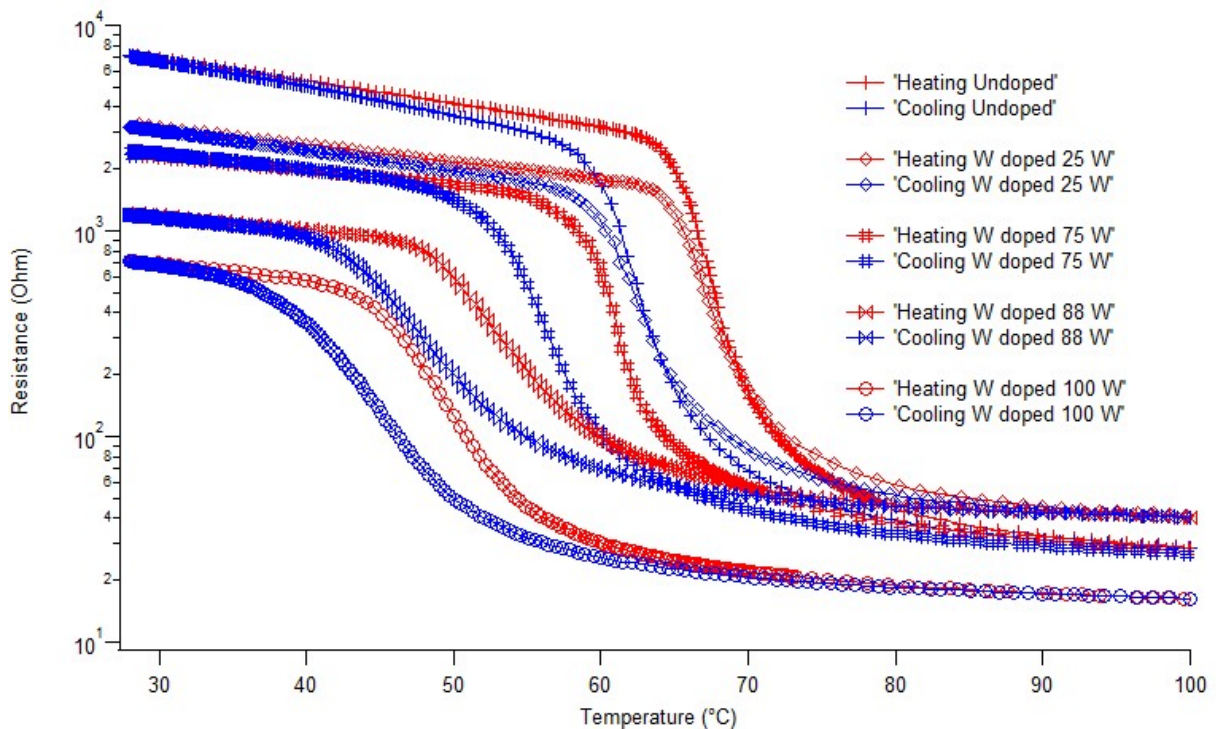
Figure 1: Temperature dependent electrical resistance of undoped and tungsten doped thermochromic films obtained by a four probe measurements. During the semiconductor-to-metal transition, the electrical resistance of undoped films undergoes a change about two orders of magnitude (logarithmic scale). The transition temperature is progressively reduced with increasing power on the tungsten target.

This result confirms undoped thermochromic films switch from semiconducting to metallic state at transition temperatures around 69°C, but tungsten doping lower the transition temperature [Goo71].

A.2.   IR imaging

At the transition there is a change not only in the structure and electrical properties , but, most importantly, a switch in the optical properties. In the IR region, the sample is transmitting in the semiconductor state and reflecting in the metallic state. This can be shown in a suggestive way with IR images taken in the cold and hot state, with a FLIR B400 thermocamera.

Sample 09.05.14
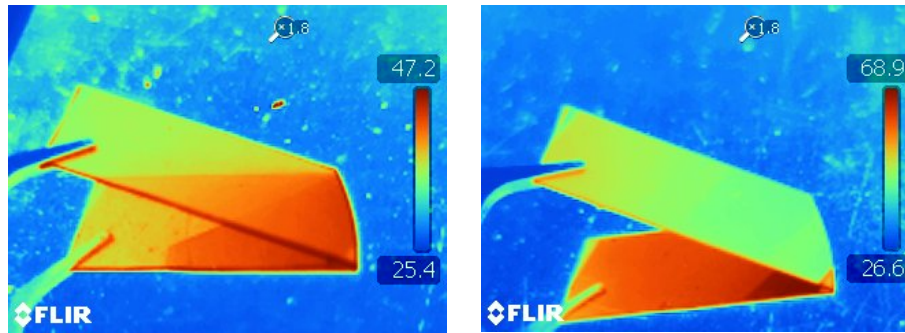
Sample 18.08.14
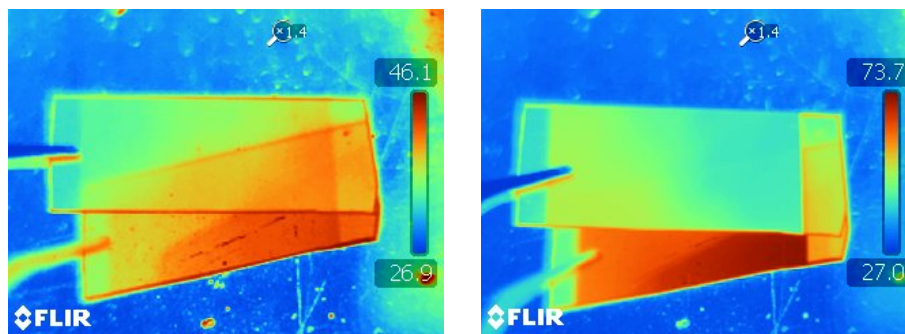
Figure 2. Infrared images of VO_2 coatings deposited on Si substrate. Semiconductor, thus transparent, in the cold state (left) and metallic, reflective, in the hot state (right)

A.3. XRD analysis of undoped and doped by tungsten thermochromic oxide coatings for phase purity confirmation

Structural information was gathered by X-ray diffraction (XRD) of thermochromic samples. Only the best switching films were analyzed by XRD. Fig. 3 shows data obtained from VO_2:W.
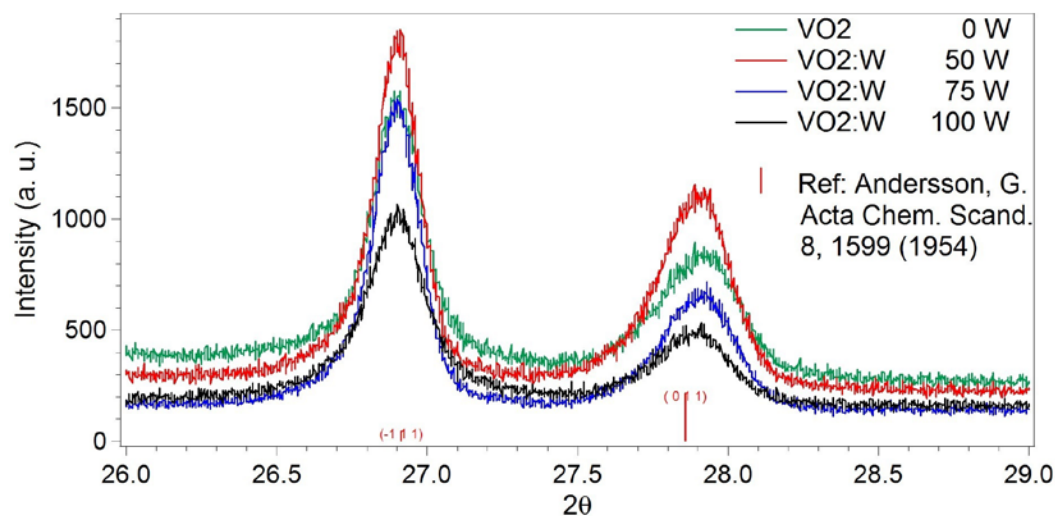
Figure 3: XRD analysis of undoped-VO_2 and VO_2:W films. In the legend is reported the RF power (in Watt) applied to the tungsten target.

The analyzed films were deposited on silicon wafers (100). The observed XRD pattern shows a correspondence with the powder diffraction data of some crystal lattice planes ([-1,1,1], [0,1,1]) of VO_2 reported in the literature [And54]. Films are well crystallized. The absence of the other peaks suggests preferential orientation of crystallites. Applying the Scherrer's formula [Cul78], a grain size of 27 nm can be estimated for VO_2.

A.4. Determination of optical constants by spectroscopic ellipsometry

Ellipsometry is a highly accurate method for investigating the optical properties of thin films. To our knowledge, only little information is available about ellipsometrically determined n and k of doped thermochromic films. For high accuracy and reliability, five different angles of reflection were used for the measurements of the ellipsometric quantities ψ and Δ in the visible and in the near infrared wavelength range, from 350 nm to 2000 nm. Four different angles were used for the measurements in the near infrared wavelength range and in the middle infrared range, from 2000 nm to 20000 nm.
A point-by-point fitting algorithm was applied in order to infer the refractive index n and the extinction coefficient k for all wavelength points λ.

Spectroscopic ellipsometry is a precise optical measurement technique working with polarized light. The method compares the ratio of the complex Fresnel reflection coefficients for parallel and perpendicular polarized light R_p and R_s. A scheme of this principle is shown in Fig. 4 (a). Fig. 4 (b) shows our FTIR ellipsometer modified with a heating stage able to stabilize the temperature of a sample during a measurement at 90°C.
This relative measurement makes the technique independent from intensity fluctuations of the source, thus favouring a high precision.

A.5. Point by point fitting for determination of the optical constants and verification by Kramers-Kronig consistent approach based on Lorentz-Drude and Lorentz-Cauchy model

n and k of a thermochromic transition metal oxide coating in the semiconducting and metallic state can be determined by fitting the measured curves point by point while changing the assumed film thickness every time. We looked for a thickness value which would minimize the root mean square error (RMSE). The initial thickness test value was found by alpha step measurements. A fine adjustment of this value was obtained fitting the measurement and looking for the thickness which best minimized the fitting error.
We adopted the Lorentz-Drude model to verify Kramers-Kronig relations in the visible and near infrared wavelength range. Lorentz-Cauchy model was chosen to verify Kramers-Kronig relations in the near infrared and middle infrared range. These relations are fundamental to confirm n and k determined by point-by-point interpolation and to physically interpret the optical properties by the band structures theory. In fact, the energy values associates to the Lorentz oscillators describe the interband and intraband optical transitions.
In Fig. 5 we report our results which are in good agreement between the n and k determined by point-by-point interpolation and those determined by the Lorentz–Drude and Lorentz–Couchy model.
According our knowledge it is the first time in literature that the optical constants of a quaternary thermochromic transition metal oxide film have been inferred in this wavelength range.
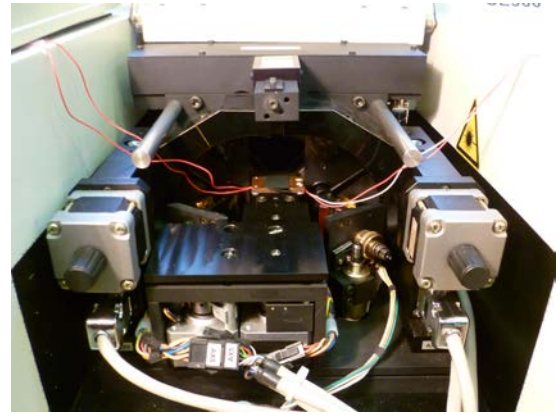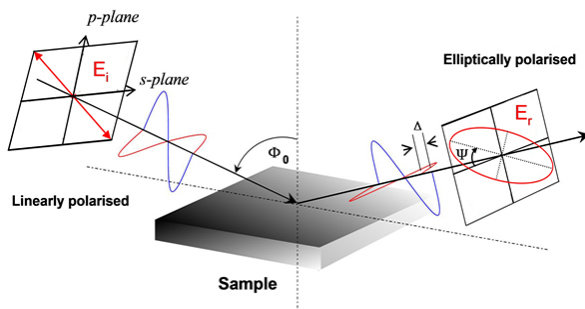
Figure 4 (a) shows a scheme of the ellipsometry principle. (b) A picture of our FTIR ellipsometer modified with a heating stage able to warm a sample during a measurement up to 90°C.

(a)   (b)
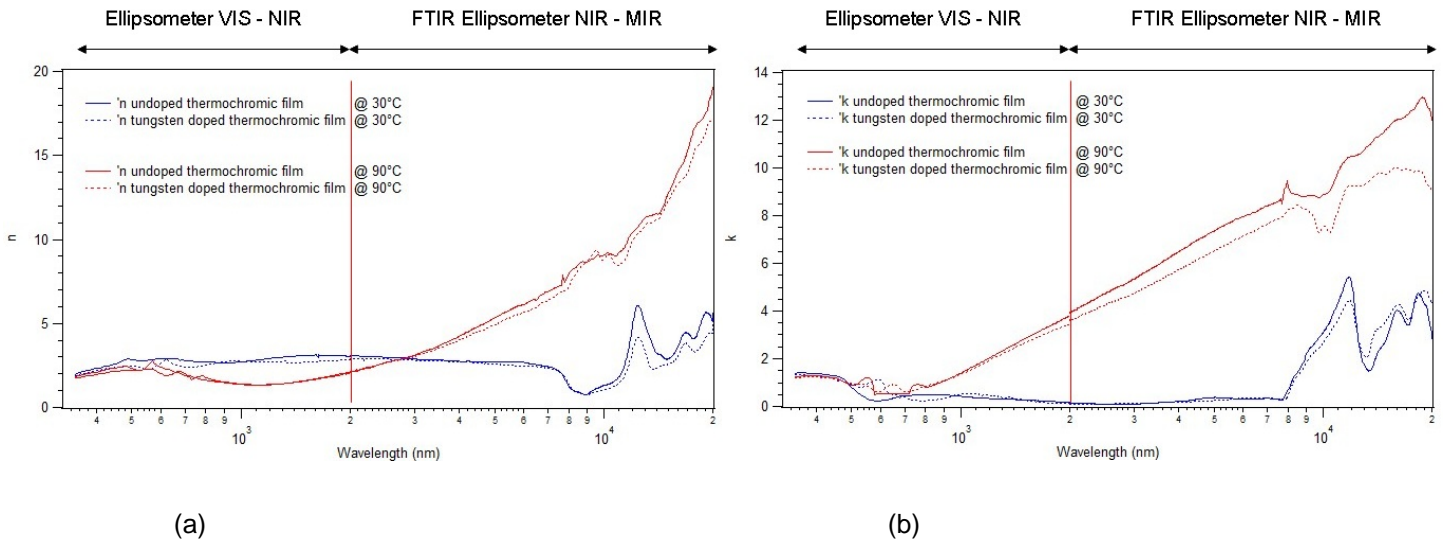
Figure 5: n (a) and k (b) for thermochromic metal oxide films undoped and doped by tungsten on sili-con wafer at around 30°C and at around 90°C determined by point-by-point interpolation.

A very reliable and consistent measurement was performed to determine the optical constants of a thermochromic transition metal oxide film. This result is remarkable especially because of the lack of these data in literature.

The optical properties of a thermochromic transition metal oxide film for both the low and the high temperature state were inferred by spectroscopic ellipsometry in the VIS-MIR spectral range. These data were used as basis for computer simulations predicting solar absorptance, solar reflectance and the thermal emittance on an aluminium substrate. The thickness of the undoped thermochromic film was varied in order to maximaze the emittance switch between the semiconducting and the metallic state.
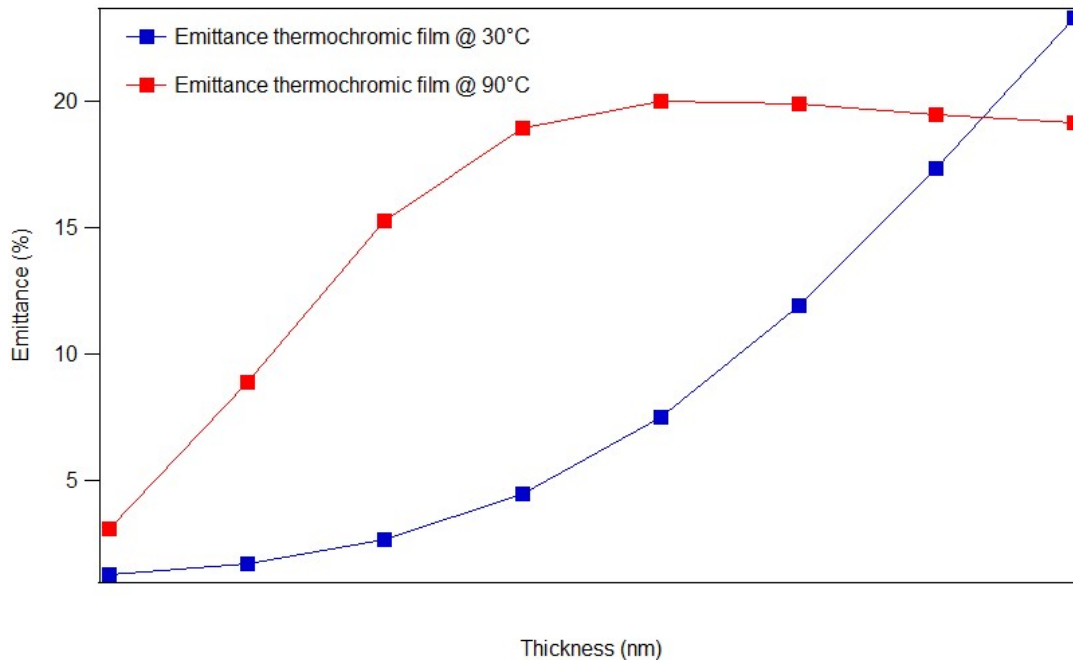
Thickness (nm)

Figure 6: Simulation of emittance switching with thickness increasing for our thermochromic film.

See Confidential appendix for further details.

Fig. 6 clearly shows the thermochromic undoped film becomes highly emissive in the metallic state. The thermal emittance is depending on the aluminium substrate at low temperature and on the metallic state of the thermochromic film after switching. The optimum layer thickness has been identified. The emittance is evaluated by integration of the absorbance spectra weighted with the thermal spectrum of a black body at 100°C. This integration was performed in the range from 2000 to 20000 nm.

This result is consistent to a preliminary theoretical prediction of our laboratory [Huo08].

A.6. *Electrical properties of thermochromic films – aluminum doping*

Aluminium doped thermochromic films were deposited once experience on co-sputtering was acquired and the best deposition parameters for doping thermochromic films were achieved.
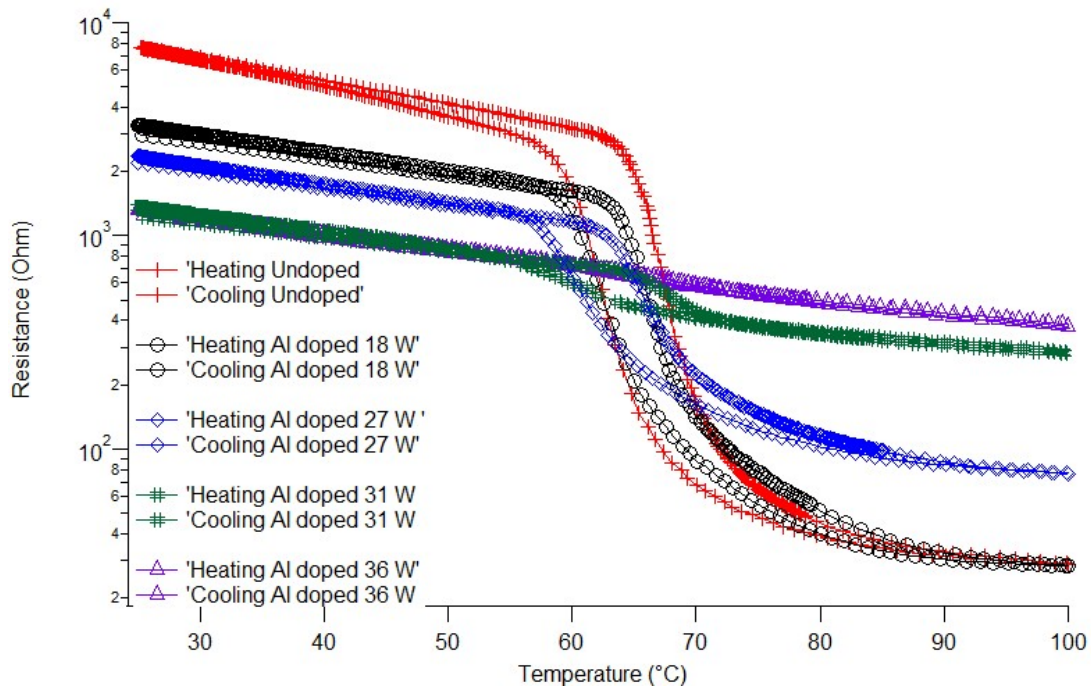
Figure 7: Temperature dependent electrical resistance of undoped and aluminium doped thermochromic films obtained by a four probe measurements. During the semiconductor-to-metal transition, the electrical resistance of undoped films undergoes a change about two orders of magnitude (logarithmic scale). This change is progressively reduced with increasing power on the aluminium target.

A.7. XRD analysis of undoped and doped by aluminum thermochromic oxide coatings for phase purity confirmation

Aluminium doping seems to make thermochromic films loosing their special peculiarity of the semiconductor-to-metal transition. It could be explained by a progressive amorphization of the film with increasing the aluminium doping.
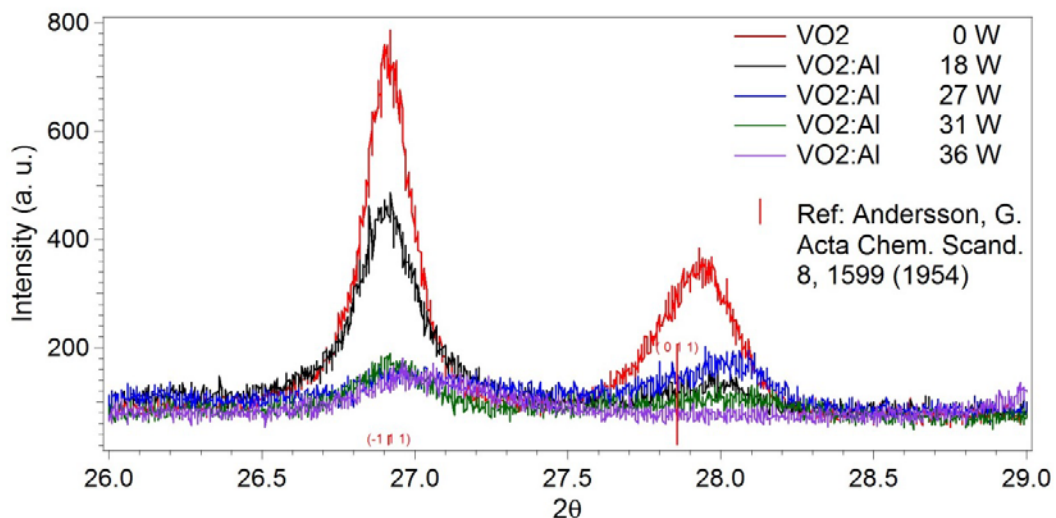
Figure 8: XRD analysis of undoped-VO_2 and VO_2:Al films. In the legend is reported the RF power (in Watt) applied to the aluminum target.

Aluminium doping makes thermochromic films loosing their special peculiarity of the semiconductor-to-metal transition. This is explained by a progressive amorphization of the film with increasing the aluminium doping. This is confirmed by the XRD results shown in Fig. 8. A progressive amorphization of VO_2:Al films occurs by increasing the aluminum doping because the intensities of these peaks decrease. A similar effect, occurs by excessive tungsten doping [Pao09].

Futhermore, literature [Goo71] suggests other suitable dopants to raise the transition temperature.

A.8. Rutherford backscattering Spectroscopy (RBS) analysis of the thermochromic transition metal oxide films for a highly accurate measurement of the film thickness and the chemical composition (doping concentration)

In Rutherford backscattering spectrometry (RBS), a sample is exposed to a beam of high energy ions. The energy of the backscattered ions allows to infer the chemical composition and the thickness of a thin film deposited on a substrate. This analysis was performed in order to quantitatively investigate the doping in the VO_2:W and VO_2:Al film deposited by RF-reactive magnetron co-sputtering.

RBS analyses of VO_2:W films produced at LESO-PB were performed at IMA-Arc (Institute of Applied Microtechnologies - La Chaux-de-Fonds) under the supervision of Dr. P. Jeanneret.

Three VO_2:W samples which show the thermochromic transition between 68°C and 49.5°C were investigated. By means of a Van der Graaff generator, a 2 MeV He^{2+} beam was generated. The scattered ions were detected with charge-sensitive "surface barrier" detectors. RBS in single shoot mode was performed on these samples. Experimental data are summarized in Tab. 1, where the power applied on the tungsten target, the film thickness and the average atomic concentration of tungsten in the thermochromic films are respectively given (relative error ± 5% at.%).

Power applied on the tungsten target (Watt)	Thickness (nm)	Tungsten (at.%)
50 W	359	0.04
75 W	365	0.12
100 W	368	0.35

Table 1: Power applied on the tungsten target, film thickness and average atomic concentration of W.

The doping concentration is inferred homogenous and reproducible. These films were deposited on a monocrystalline silicon wafer.

As for the results of the chemical analyses of the thermochromic film deposited by thermal evaporation in 2010, these findings suggest that tungsten doping of our VO_2 films is more effective (doping efficiency of -55°C/at.% ± 12%) than previously reported in literature (doping efficiency of -23°C/at.%) [Sol06]. Instead of occupying the sites in the crystal lattice where they contribute to lowering the transition temperature, most of the tungsten atoms might segregate into an eventual second tungsten-rich phase.

The atomic concentrations of Al was estimates less than 2% in every VO_2:Al film. A precise quantitative determination of this doping is not possible by RBS analyses due to the detection limits of this technique. By RBS, a heavier dopant into a lighter matrix can be more precisely determined instead of a lighter element into a heavier matrix because the probability of interaction between the dopant and the ions of the beam is related to their atomic masses.

A.9. Electrical properties of thermochromic films – D1 doping

Samples with different doping content were measured and compared. The doping level was varied by applying different power on the dopant target: 10, 20, 30, 50, 60 and 70. For each doping level, the samples showing the best transition were selected.
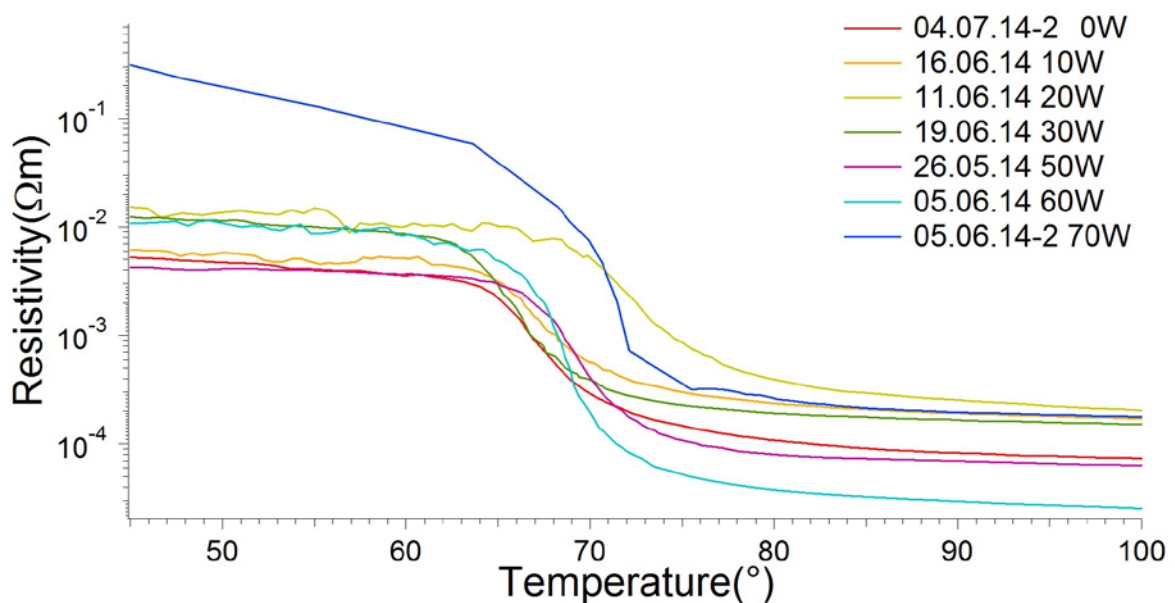
Figure 9: Resistivity measurements of undoped and D1 doped samples. In the legend the power applied on the dopant target is reported

The transition temperatures were the following:

Sample 4.07.14-2 T_C = 67.7 ± 0.5°C
Sample 16.06.14 T_C = 66.9 ± 0.5°C
Sample 11.06.14 T_C = 72.4 ± 0.5°C
Sample 19.06.14 T_C = 66.0 ± 0.5°C
Sample 26.05.14 T_C = 69.6 ± 0.5°C
Sample 05.06.14 T_C = 68.6 ± 0.5°C
Sample 5.06.14-2 T_C = 69.0 ± 0.5°C

There was no observable trend resulting from D1 doping. There were two samples (16.06.14 with 10W and 19.06.14 with 30W) with slightly lower transition temperature than the reference, but still in the range where pure VO_2 switches suggesting that the doping level could have been too small to show any effect and the measured temperature is that of pure VO_2. However, sample 11.06.14 with only 20W applied power on the dopant target showed the second highest T_C of 72.4 ± 0.5°C. This could mean that, while D1 might have some effect on increasing the transition temperature, in some cases (16.06.14, 19.06.14) it fails to enter into VO_2 lattice, while in other cases (11.06.14) it does. This can

be due to various reasons, not only the doping level. It might be related to temperature variations in the chamber, which influences the surface diffusion.

However, when the doping level is increased considerably, the D1 is forced to enter the lattice and for the last three samples, 05.06.14 with 60W and 05.06.14-2 with 70W, an increase of the transition temperature with doping level can be noticed.

Although, our results suggest the possibility of increasing the temperature by D1 doping, the temperature is only increased slightly even at high levels of doping.

We attribute the non-consequent behaviour of D1 doped samples, to a possible segregation of the D1 in the film, being very difficult to insert the D1 in the lattice. This is suspected because of heavy flake formations in the deposition chamber and because of different resistivity results from different points of the same samples. This suggest that in some parts D1 manages to accommodate in the VO_2 lattice, while in others not.

An interesting aspect is that, although by doping usually the step of the transition decreases significantly, for D1 doping, the step of transition was comparable to that of the reference sample, in some cases being even bigger. This is important because, even if the gain in the transition temperature is not so large, the transition step it is not lowered and there are no losses in its magnitude, exhibiting the same sudden change in electrical and optical properties than pure vanadium oxide films.

A.10. SEM analyses

For same doping level, some of the samples exhibited a hazed surface while others were completely homogeneous. We investigated these samples with scanning electron microscopy to have a better understanding of the film morpholgy.

Samples 26.05.14 and 27.05.14-2, both being doped by applying 50W on the D1 target, were analyzed. The only difference between the two samples was the O_2 partial pressure, all other parameters being held constant.

- Sample 26.05.14:   initial O_2 flow 2.77 sccm
  final O_2 flow 2.75 sccm
- Sample 27.05.14-2:   initial O_2 flow 2.72 sccm
  final O_2 flow 2.66 sccm
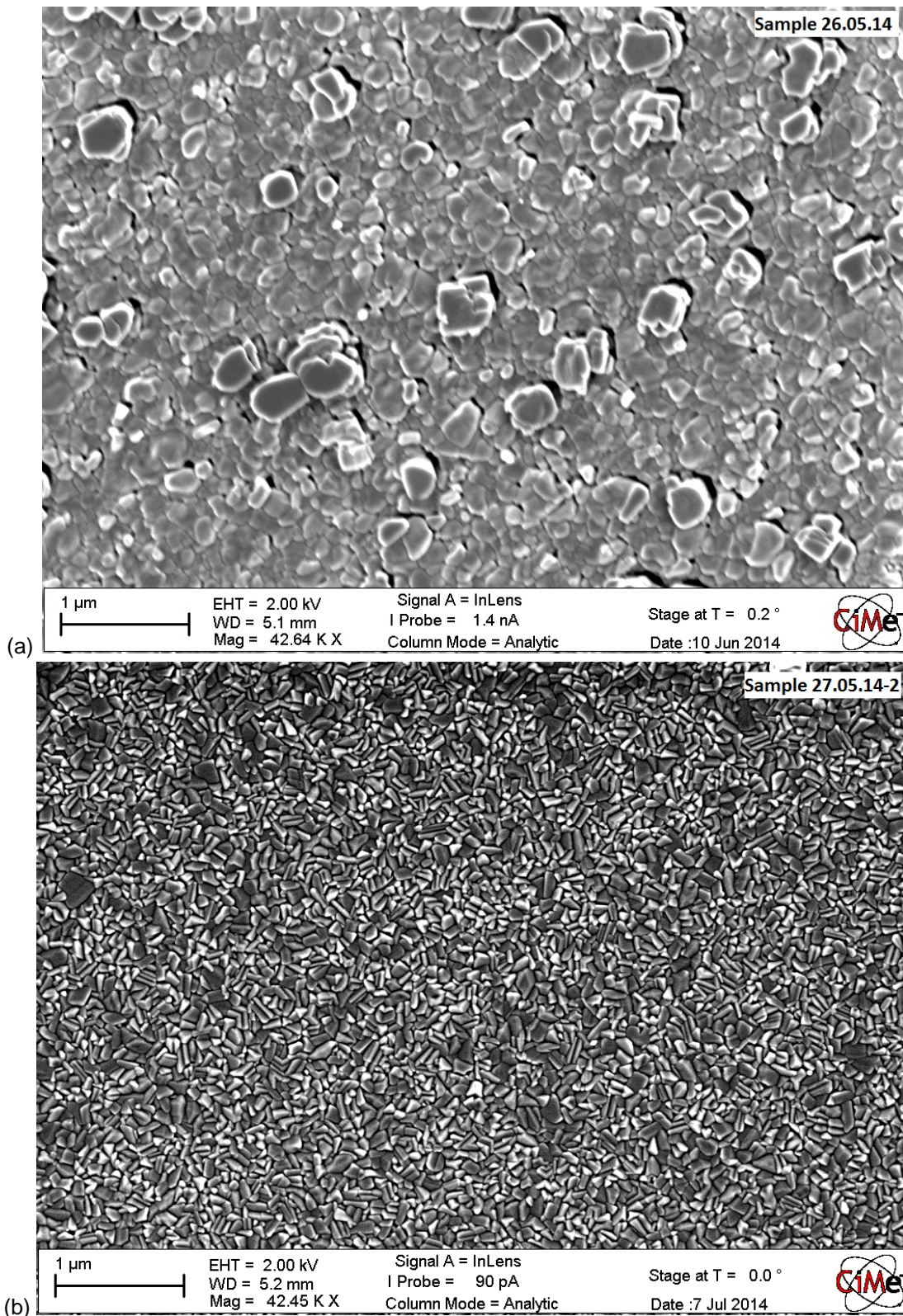
Figure 10:(a) and (b). SEM images of hazed sample 26.05.14 and homogeneous sample 27.05.14-2 having the same D1 content

The SEM analyses showed that the hazed sample had different film morphology than the homogeneous one. For sample 26.05.14 the grains were rounded in shape and showed a multidisperse grain size distribution. It is energetically favoured that big grains grow on the expense of small ones, as the surface energy is lowered. This thermodinamically driven phenomenon is called Ostwald ripening. When the grains grow and reach sizes comparable to the wavelength of visible light,

it will scatter the light resulting in hazed samples.

The homogeneous sample 27.05.14-2 shows almost monodispersed grain size distribution, with slightly acicular grains. The grains are smaller than the 600 nm so the film does not scatter visible light.

The changes in morphology are significant and were induced only by a slight change in O_2 partial pressure. The O_2 flow was almost constant for sample 26.05.14, the sample should be single phased, whereas for 27.05.14-2 the flow varied.

A.11. Reflectance in visible

Total and diffuse reflectance of a hazed (26.05.14) and homogeneous (27.05.14-2) sample were measured. The total reflectance spectrum, as expected, has the same shape for both samples, the only difference being the value of the reflectance. In the hazed sample, due to higher absorption, the value of total reflectance is lower, amounting to a maximum of ~ 20% at 430-450 nm, whereas in the homogeneous sample there is less absorption and the reflectance is ~ 27% in the same wavelength range.
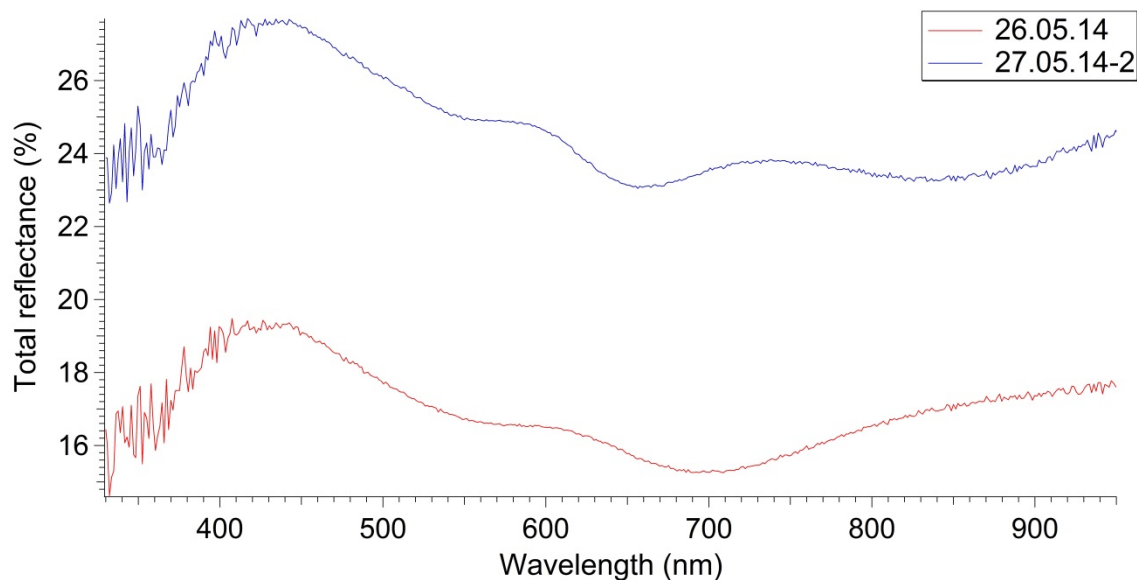
Figure 11: Total reflectance spectrum of a hazed (26.05.14) and unhazed (27.05.14-2) sample.

When measuring the diffuse reflectance, the spectra are very different for the two samples. In case of the hazed sample there is a steep decrease in diffuse reflectance from about 440 nm to 850 nm, while the homogeneous sample exhibits no change and the values are very low. The slope of the diffuse reflectance spectrum of the hazed sample decreases as a function of $1/(\lambda^4)$, which means that Rayleigh scattering occurs in the film. This result is in accordance with the SEM measurements, where the difference in morphology between the two samples was outlined. This confirms that the grains in sample 26.05.14 are comparable in size with the wavelength of visible light and they are responsible for the occurance of haze in the film.
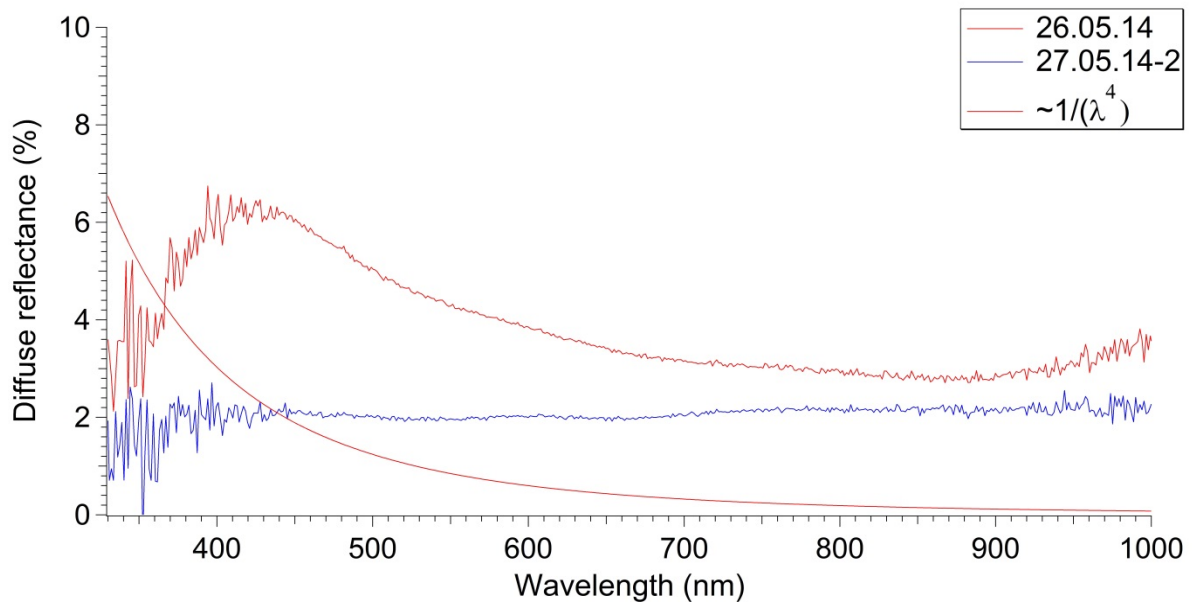
Figure 12: Diffuse reflectance spectrum of a hazed (26.05.14) and unhazed (27.05.14-2) sample and the typical slope of Rayleigh scattering

A.12. Transmittance in IR

Transmittance of D1 doped VO_2 films, in the near infrared range, was measured. The transmittance spectrum of the semiconducting state was determined at room temperature, while for measuring the metallic state, the sample was heated up to $\sim 90°C$. The maximum transmittance observed is 16% at 2000 nm for the Si wafer covered by the thermochromic coating. When heated, the thermochromic layer switches, becomes reflective and transmittance becomes 0. Changes in transmittance can be noticed only in the infrared range, because Si is opaque in the visible range.
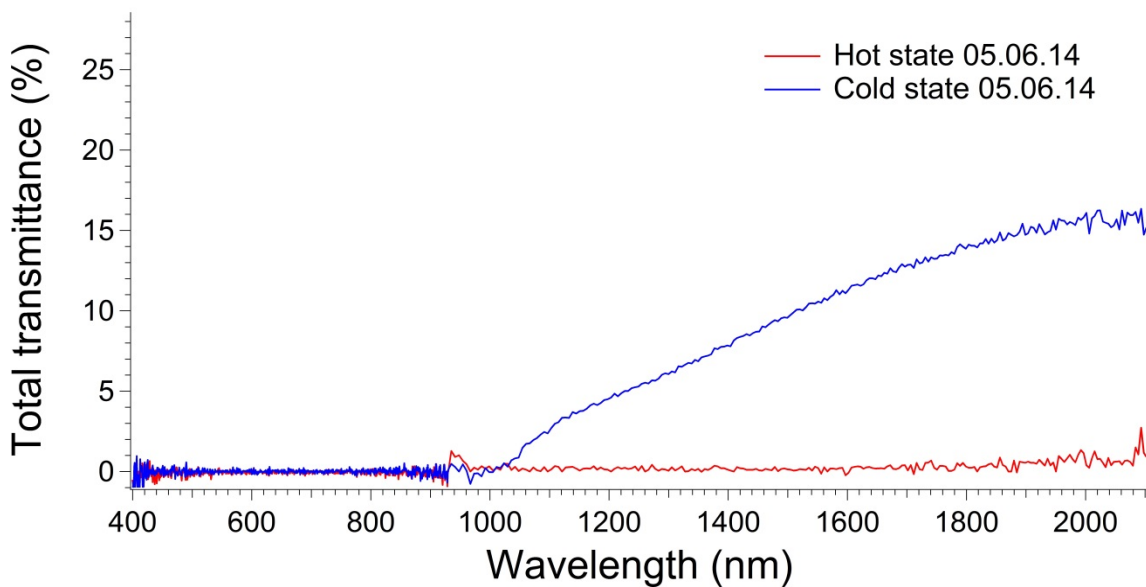
Figure 13: Transmittance of a switching VO_2:D1 film on silicon substrate.

A.13. Electrical properties of thermochromic films – D2 doping

Samples doped with D2 by applying 10, 20 and 30W power on the dopant target were compared. Except the power on the D2 target, all other parameters were held constant.
See Confidential appendix for further details.

Sample 18.08.14 has T_C = 73±0.5°C,
Sample 19.08.14 has T_C = 76±0.5°C,
Sample 21.08.14 has T_C = 86±0.5°C,
Sample 22.08.14 showed no transition.

A.14. EDX and ESCA measurements

Energy-dispersive X-ray spectroscopy (EDX) is a useful technique for determining chemical composition. EDX measures spectra of X-rays emitted by a sample which is irradiated by high energy electrons. Excited atoms loose energy by emitting characteristic X-rays. Each element has a unique atomic structure allowing unique set of peaks on its X-ray spectrum, this feature allows to analyze the composition of a sample.
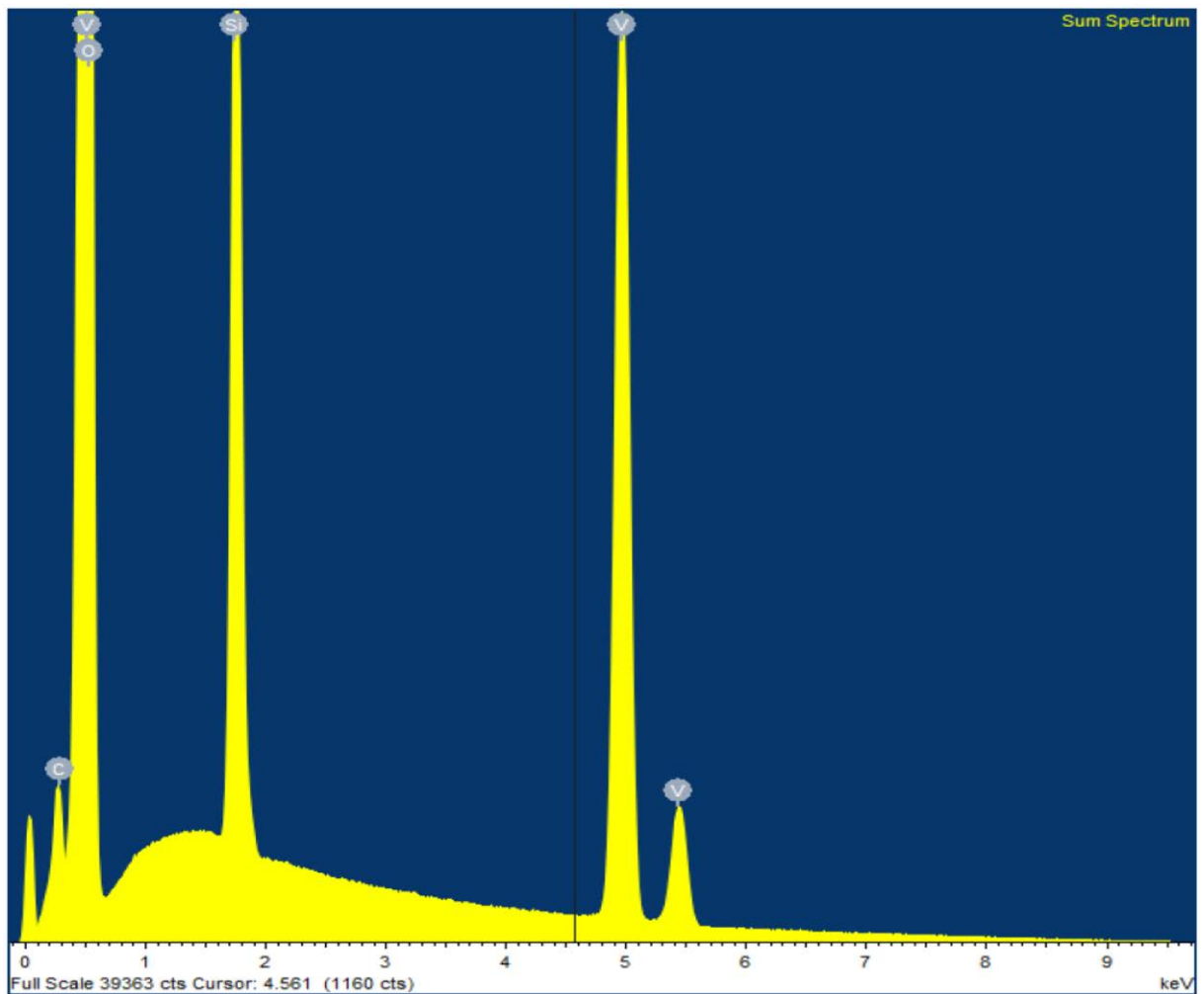
Figure 14: EDX spectrum from 0 KeV to 9.7 KeV of a VO_2 sample.

In situ ESCA measurements were carried out on D2 doped vanadium oxide films. Although, switching films were not obtained, it was possible to determine the regions where the D2 and vanadium valence and Auger peaks occur. The survey scan is presented in the confidential appendix, while the spectrum of the region which includes the peaks related to V 2p and O1s is presented in Fig. 15. Furthermore, a quantification of these elements was done and it was determined that applying 10W power on the dopant target corresponds to approximately 1 at.% D2 doping.

The reason why switching VO_2 films have not been deposited, was that the substrate temperature was not at the right height in the sputtering chamber. For ESCA measurements a different sample size and sample holder is required. To determine the optimum deposition temperature for the new sample holder, which conducts differently than the previous one, is time consuming and until the end of this project it was not found.
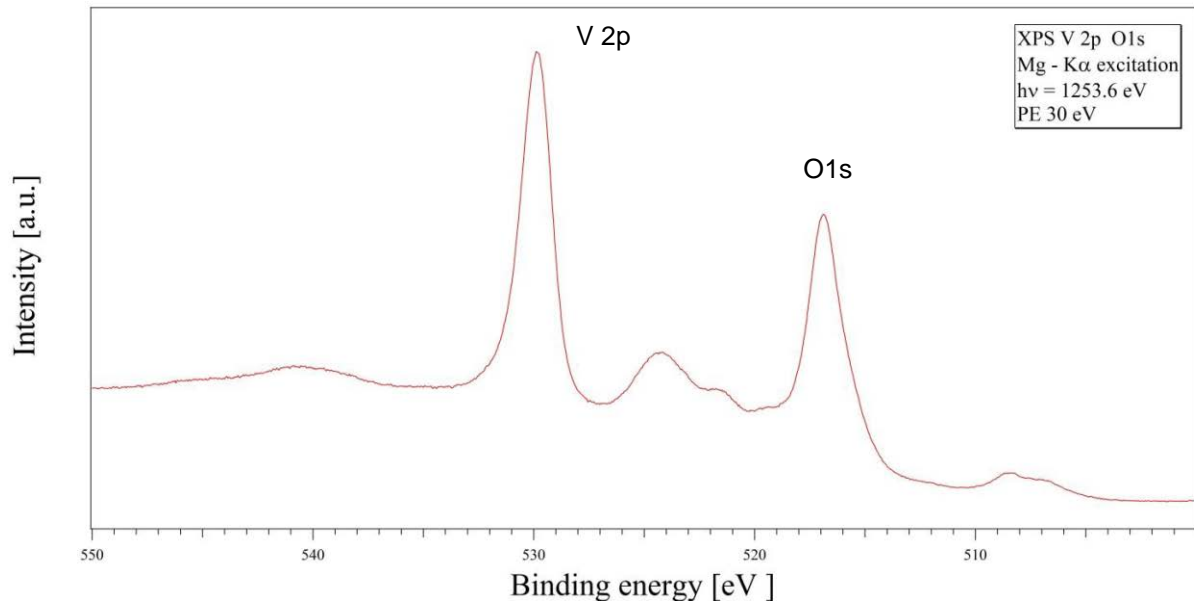
Figure 15. XPS spectrum from 550 eV to 500 ev of a VO_2 sample.

B. Simulations for determining optimized multilayer designs for switching coatings

Keeping constant the thickness of the thermochromic film relative to the highest emittance switch, the optical performance of an optimized multilayer composed by the switching coating and an antireflection film deposited on top was simulated in both temperature states. The thickness of the antireflection coating was optimazed in order to minimize the solar reflectance.

Simulations were performed for a thermochromic film doped by tungsten as well. Fig. 16 shows a simulation of reflectance switching of an optimized multilayer composed by a thermochromic film doped by tungsten and an antireflection coating.
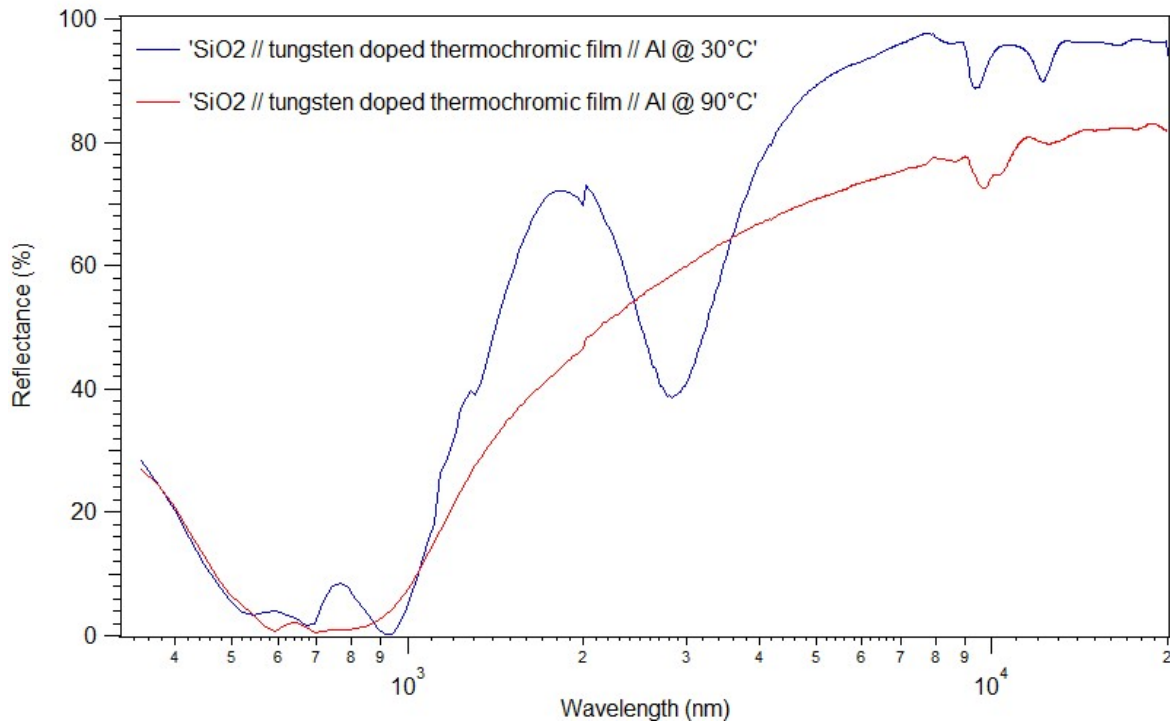
Figure 16: Simulation of reflectance switching of an optimized multilayer deposed on an aluminum substrate composed by a thermochromic film doped by tungsten and an antireflection coating.

See Confidential appendix for further details.

By means of computer simulations, a promising multilayer design for thermochromic selective absorber coatings was identified.

The specular reflectance of doped and undoped thermochromic films was measured by FTIR spectrophotometry in the spectral range from 2000 nm up to 20000 nm. We used the optical constants found by ellipsometry to simulate the optical reflectance of these films. A very good agreement between the measured spectra and the simulated ones was found, but it is not showed in this short report.

The solar absorptance was inferred from the optical data.

C. Computer simulations of solar thermal energy systems

C.1. Stagnation temperature of a collector adopting a switching thermochromic absorber

The optical properties of a thermochromic transition metal oxide film for both low and high temperature states have been previously inferred by spectroscopic ellipsometry in the VIS-MIR spectral range. These data are used as basis for computer simulations predicting solar absorptance and the thermal emittance on an aluminium substrate.

The model of the solar collector which was adopted for this simulation is reported in Fig. 17 (a). In Fig. 17 (b), the stagnation temperature for a thermochromic film mixed with a 40% volume fraction of SiO_2 is reported. This figure clearly shows the doped thermochromic film becomes highly emissive in the metallic state. The thermal emittance is depending on the aluminium substrate at low temperature and on the metallic state of the thermochromic film after switching. The optimum layer thickness has been identified. The emittance is evaluated by integration of the absorbance spectra weighted with the

thermal spectrum of a black body at 100°C. This integration was performed in the range from 2000 to 20000 nm.

Baldi *et al.* [Bal08] calculated this stagnation map on the method described by de Vries [Vries98] and Zondag *et al.* [Zon03]. They considered the absorber as a single layer without taking into account the substrate. A solar absorptance of about 0.75 was obtained in the semiconducting state by using the thermochromic film mixed with a 40% volume fraction of SiO_2. The absorbance increase in the metallic state is not negligible. A solar absorptance of about 0.86 was obtained in the metallic state.

The glycols used in solar thermal collectors start to degrade above 170°C, the use of this coating as solar absorber lowers the stagnation temperature below this critical point. In this simulation the antireflective coating of SiO_2 was not considered.
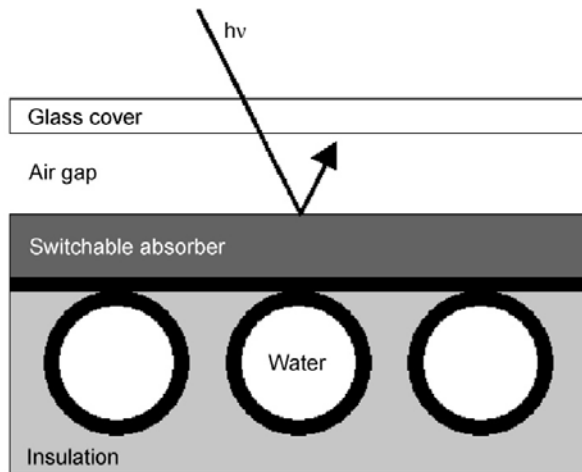
Fig. 17 (a): Model of the solar collector.
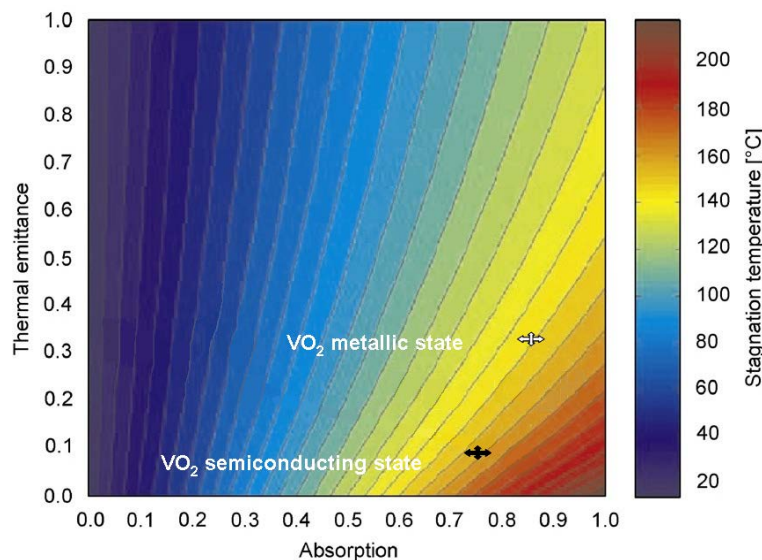
Fig. 17 (b): Stagnation temperature map as a function of solar absorptance and thermal emittance of a VO_2 based absorber of the model of the solar collector showed in [Bal08]. The arrows indicate the stagnation temperature for a thermochromic film mixed with a 40% volume fraction of SiO_2, both in the metallic (white arrows) and semiconducting (black arrows) states.

C.2. Determination of the produced energy as a function of the thermochromic transition temperature

In order to evaluate the influence of the switching temperature of a thermochromic absorber on the total energy produced by a dynamic collector, a thermal system including the COBRA Soltop panel was considered. The loss of energy due to two switching temperatures, 68°C and 95°C, was estimated in the "worst case scenario" considering an ideally perfect thermochromic absorber with a solar absorption switching from 95% to 0%.

The maximum daily temperature of the COBRA Soltop collector was determined by PolySun simulations according to the requirements summarized in the following figure:
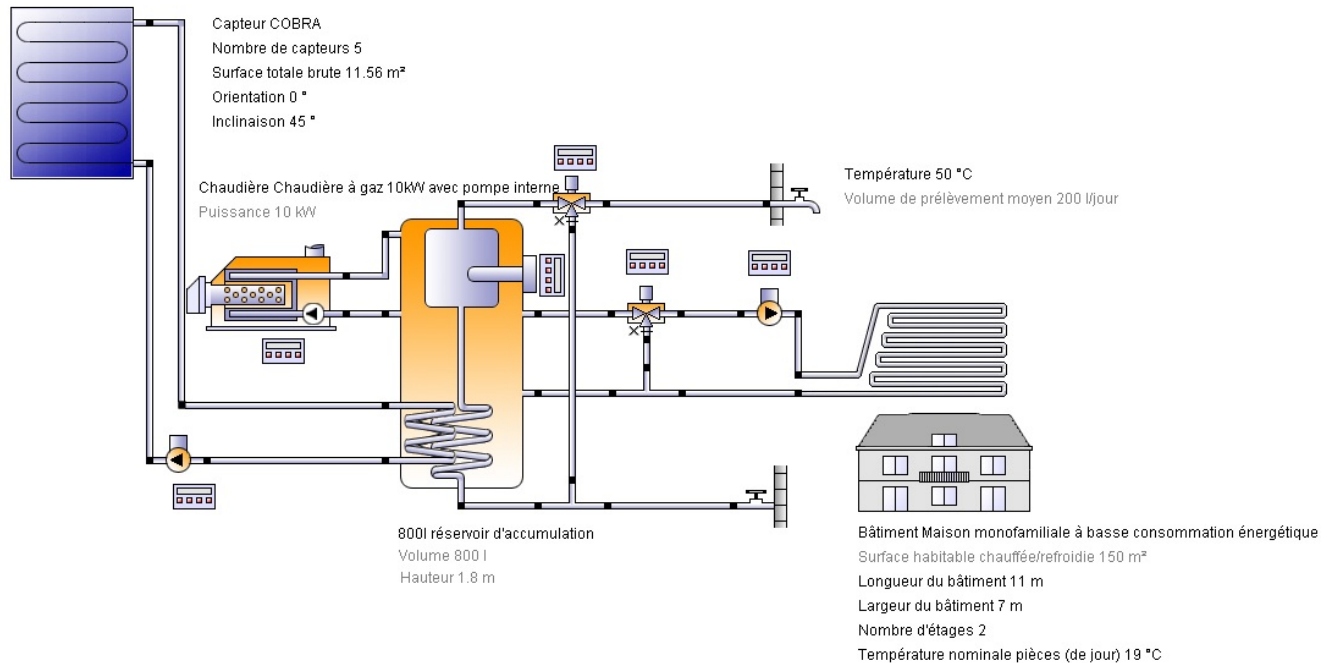
Figure 18 (a): Thermal installation located in Lausanne. 5 solar panels COBRA type were simulated in combination with a 10 kW gas boiler in order to provide 200 l/day at 50°C for domestic use and to heat a 150 m^2 residential building.

COBRA : total collector output : 4496 kWh
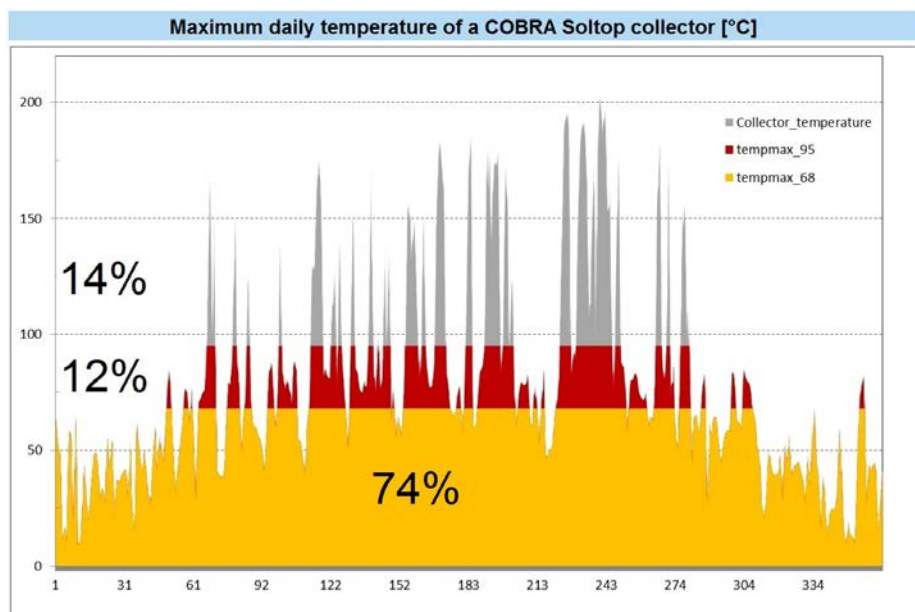
Figure 18 (b): The maximum daily temperature of a COBRA Soltop collector. The yellow and the red area represent the energy produced when the temperature of the absorber is respectively below 68°C and between 68°C and 95°C.

The thermal installation is located in Lausanne. Fig. 18 (b) shows the performance of this collector. The yellow, the red and the grey area indicate respectively the energy produced by the absorber when its temperature is below 68°C, between 68°C and 95°C, and above 95°C.

In Fig. 18 (b), the solar absorption and the thermal emittance of the simulated absorber are written on the right side of the figure.

If a hypothetic thermochromic absorber with a solar absorptance α switching between 95% and 0% would be used instead of a static absorber, the produced energy depends on the switching temperature, T_C. Such a thermochromic solar absorber would lower the stagnation temperature below the critical degradation temperature of the glycols (170°C), and also below the temperature of water evaporation (100°C).

The thermal energy which would be transferred to the thermal energy system corresponds to either the yellow area of Fig. 18 (b) (for T_C = 68°C) or to the red + yellow area (for T_C = 95°C). The yellow, the red + yellow and the grey areas comprise respectively 74%, 86% and 14% of the total area. Using such thermochromic absorber with a complete switch in the solar absorptance and a transition temperature of 68°C, 12% of the total energy would be lost with respect to a transition temperature of 95°C. However, this comparison is an overestimation of the losses, because it is based on the assumption on a complete shutdown of delivered energy. For real thermochromic absorber coatings, the delivered energy is not shut off completely (as is e.g. the case for coatings switching predominantly in thermal emissivity).

D. Thermal coupling of coating on absorber sheet and glazing

Combining a thermotropic glazing with a thermochromic absorber could protect the solar thermal collector more efficiently from overheating. In this section, the possibility to trigger a dynamic glazing by of the rise of emissivity of the absorber will be discussed.

Thermotropic glasses change transmittance when their temperature rises by increasing opacity. For our thermochromic absorber coatings, the thermal emissivity increases as soon as the transition temperature is reached. In this situation, we expect that the temperature of the thermotropic glass rises, too, triggering thereby the thrmochromic or thermotropic transition which causes a decrease in solar transmittance.

The aim of this study is to calculate the temperature change of the covering glass pane. The temperature rise of the thermochromic/thermotropic glazing has to be sufficiently high in all weather conditions. The wind speed and the ambient temperature have to be taken into account as they affect the heat transfer towards the surroundings.

D.1. Thermal coupling with single glazing - Introduction

$$\varepsilon_{abs}$$
$$T_\infty$$
$$T_{glass}$$
$$d$$
$$H$$
$$\tau$$
$$T_{abs}$$

T_∞	ambient temperature
T_{glass}	cover glass temperature (thermotropic)
T_{abs}	absorber temperature
ε_{abs}	absorber emissivity (will vary with T_{abs})
τ	roof slope
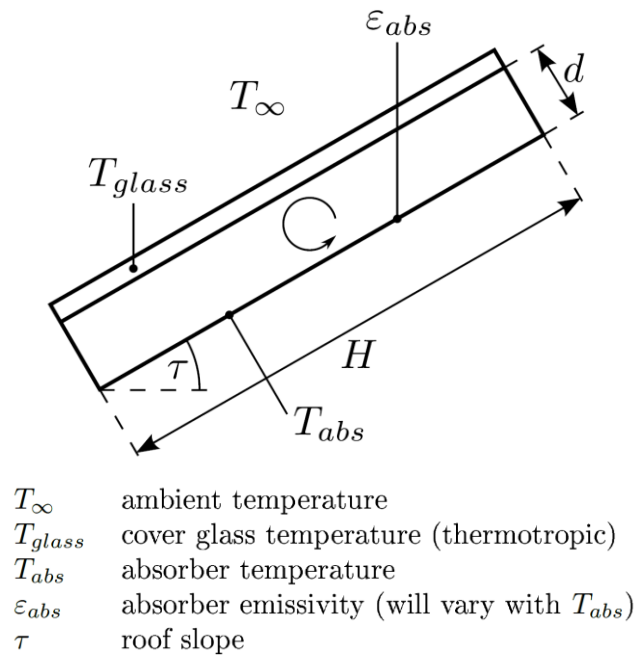
Figure 19: Schematic drawing of the solar thermal collector.

For this study we fill fix the following parameters:

$$
\begin{aligned}
H &= \text{2 meters} \\
d &= \text{2 centimeters} \\
\tau &= \text{30deg} \\
\varepsilon_{glass} &= 0.837
\end{aligned}
$$

The absorber is thermochromic. So the emissivity changes with the temperature. Following parameters have been considered:

$$
\begin{aligned}
T_{abs} < 64°C &\Rightarrow \varepsilon_{abs} = 0.05 \\
T_{abs} > 95°C &\Rightarrow \varepsilon_{abs} = 0.5
\end{aligned}
$$

These conditions correspond to the modes of normal low temperature operation and overheating. In the temperature range between 64°C and 95°C the thermochromic absorber coating might already have been switched, but the additional transition of the thermochromic/thermotropic glazing is not yet necessary.

The goal is to estimate how the glass temperature is correlated with the ambient temperature and external heat transfer coefficient h_{ext}.

2D simulations
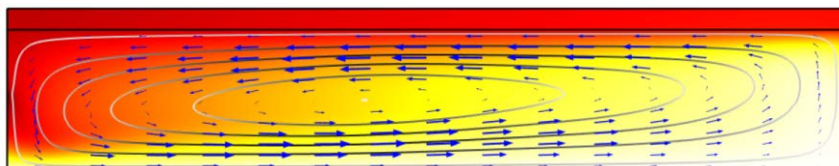
Figure 20: simulation of convection in tilted rectangular enclosure with COMSOL Multiphysics.

Finite element computer simulations of complex fluid dynamics were performed with COMSOL Multiphysics in order to evaluate the heat transfer between to absorber sheet and the glazing.

In the complex simulations of a full solar collector, the following difficulties were encountered:
- Long computing times
- Problems of convergence of the computing algorithm (occasionally)
- Varying number of convection loops leading to uncertainty in the results

However, the external heat transfer coefficients were determined with COMSOL. The values chosen for the rest of the study are given in Table 2.

h_{ext} [W/m^2 K]	wind speed [m/s]
8	1 ± 0.5
23	5 ± 0.5
46	9 ± 0.5
200	44 ± 2

Table 2: External heat transfer coefficients as a function of wind speed.

1D simplification

A node model was used to describe the system. The diagram in Fig. 21 shows the equivalent electrical circuit of the system:
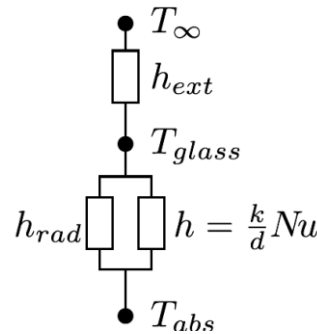
Figure 21: Simplified 1D thermal model of the solar collector.

Radiation, convection and conduction heat transfer coefficient were determined using the corresponding formulas [Fai91]. Convection formula was chosen in accordance to the geometry of the design, e.g. tilted rectangular cavities [IDW].

An analytical approach allowed us to determine the glass temperature by iteration.
The thermal flux is constant through the system therefore it is equal at the nodes before and after the glass.

$$h_{ext} \cdot (T_{glass} - T_\infty) = (h_{rad} + h) \cdot (T_{abs} - T_{glass})$$

therefore

$$T_{glass} = \frac{T_\infty \cdot h_{ext} + T_{abs} \cdot (h_{rad} + h)}{h_{ext} + h_{rad} + h}$$

In order to solve this equation, an iterative method is adopted. Firstly, an estimation of T_{glass} is

necessary, then a new T_{glass} is calculated. Reusing the last result of T_{glass} as improved approximation, this iteration is repeated until the value converges.

In each of the three cases of external heat transfer coefficient h_{ext}, the glass temperature T_{glass} was calculated in two configurations. For a low absorber temperature with $T_{abs} = 64°C$ and $\varepsilon_{abs} = 0.05$ and for a high absorber temperature with $T_{abs} = 95°C$ and $\varepsilon_{abs} = 0.5$.
The switching temperature of the thermochromic/thermotropic glazing has to lie in the interval between the glazing temperatures obtained for these two cases.
The range of suitable transition temperatures of the thermochromic/thermotropic glazing has been identified for this situation. The detailed results are given in the confidential annex of this report.

D.2. Thermal coupling with single glazing - Results

The external heat transfer coefficients were determined with COMSOL Multiphysics. The values chosen for the rest of the study are given in Table 2. In order to infer the glazing temperature as function of the external temperature and h_{ext} an analytical approach was preferred. The results are given in Fig. 22.
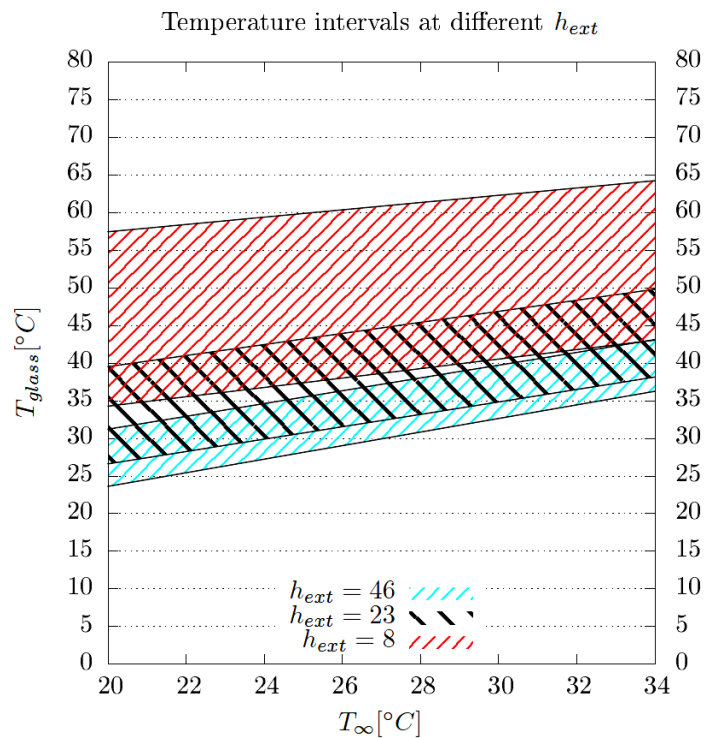
Figure 22: Glazing temperature in varying conditions of the external temperature and h_{ext}.

Fig. 22 shows the glazing temperature for different wind conditions. The light gray part represents wind at 1 ± 0.5 m/s ($h_{ext} = 8$ W/m^2 K), the black one wind at 5 ± 0.5 m/s ($h_{ext} = 23$ W/ m^2 K), and the dark gray one wind at 9 ± 0.5 m/s ($h_{ext} = 46$ W/m^2 K).
For T_∞ between 23°C and 34°C and the considered range of wind speeds, a switching temperature of 41°C is suitable for triggering the transition of the thermochromic glazing. In fact, with a switching temperature of the thermochromic glazing of 41°C, the transition of the thermochromic absorber would trigger the transition of the thermochromic glazing for values of $h_{ext} \leq 23$ W/m^2 K (wind at less than 5 ± 0.5 m/s) in the range of T_∞ between 20°C and approximately 32°C. This means that for the latitudes of central Europe, the triggering mechanism of a single glass collector would work in a very wide range of conditions. During summer, with a $T_\infty > 32°C$, the thermochromic glazing would be in its opaque

state without any trigger, but equally avoiding the overheating state. During windy days (wind at more than 5 m/s) and/or during winter, the thermochromic glazing would be in its clear state, therefore, without guaranteeing the overheating protection. This represents a minor drawback because during winter the overheating problem of a thermal solar collector is a remote eventuality.

D.3. Alternative concept: collector with double glazing

In order to improve the thermal coupling between absorber and glass pane, a second glass can be added to reduce the external conductive heat transfer towards the exterior.
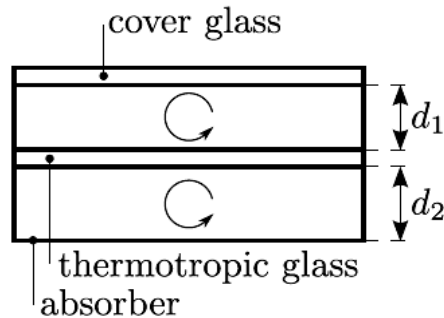
Figure 23: Collector with double glazing.

The distances d_1 and d_2 are fixed to 2 centimetres. This distance minimizes the heat transfer in double glazing.

As in the first case, a 1D reduction has been used. The diagram in Fig. 24 represents the equivalent electrical circuit.
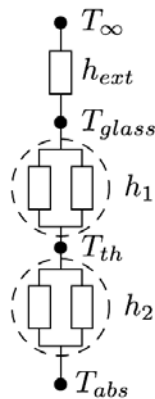
Figure 24: Simplified thermal model for the collector with double glazing.

Two temperatures must be estimated: T_{th} and T_{glass} . Since the heat flow is equal at each node we can use the rule to add two serial conductances to obtain the result.

The range of suitable transition temperatures of the thermochromic/thermotropic glazing has been identified for this situation. The result of the calculus is presented in Fig. 25.
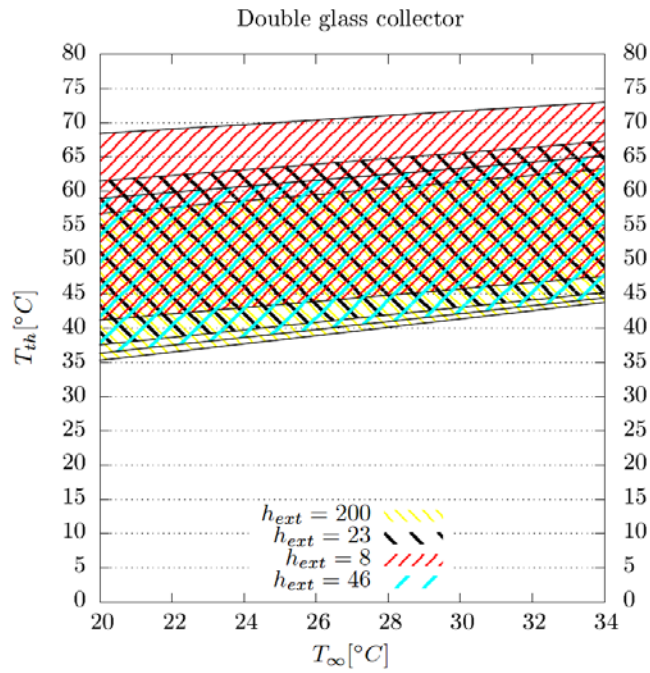
Figure 25: Glass temperature in the double glazing case.

In the case of a double glazing (see Fig. 25), the thermal coupling between the solar absorber and the inner glass pane is improved. The temperature of the inner thermochromic glazing follows more closely the temperature of the solar absorber. In addition, a better thermal insulation of the collector is provided. However, double glazing reduces somewhat the optical efficiency and adds cost and weight to the total system. A double glass collector would work in any conditions for latitudes of central Europe. In both cases, the efficiency of the switch depends only from the solar transmittance below and above the transition temperature.

E. Switchable coatings on the collector gazing

E.1. Study of available products on the market

Dynamic glazing - also called smart glazing or smart glass – changes its properties depending on different parameters. This project deals mainly with a thermochromic coating; it changes its colour with the increase of temperature in order to switch absorptance and emissivity. Other types of dynamic coatings include, electrochromic and electrotropic glazing, changing respectively its colour or opacity, depending on the applied current. As the aim is to implement this coating on the glazing of a solar collector, a passive solution would be preferable. Having this purpose in mind, thermotropic coatings were investigated. Thermotropic coatings change opacity when their temperature rises above a given threshold. Therefore, an increase of the temperature of the solar absorber and its switch in emissivity would trigger the thermotropic coating, which would prevent the solar collector from overheating by increasing opacity.

The development of smart glass sector is currently at its early stage. More and more types of products appear or are improved but the market volume is low. Due to their price and questions about longevity, reliability and system integration, they are not yet in everyday use. On the other hand, buildings and even automotive use more and more glass and energy demand is a major concern. More recently, switchable mirrors using Chiral Liquid Crystals have been developed. This technology is emerging but its commercialization is still in progress. A study made by Navigant Research in 2013 [NAV13] estimates an important growth of the market volume for electrochromic, suspended particles,

thermochromic and photochromic glass by 2022. Nevertheless, the latter study does neither consider thermotropic glass nor switchable mirror.

Even if sales volumes are small, electrochromic and electrotropic glazing already exists quite widely on the market. Due to the ease of changing the state with an electrical switch, they are used in a small domain for light control or privacy. Therefore, this type of glazing is often called privacy glass.

Main manufacturers include:

- o Electrochromics, SageGlass™
- o Innovative glass, LC Privacy glass
- o Polytronix, Polyvision™ switchable privacy glass
- o Research Frontiers, SPD SmartGlass

A thermotropic glass becomes opaque when the temperature rises above a given threshold. A Japanese company called Affinity developed a product called Thermotropic Smart Windowpanes. Some windows have been produced with the Technical University of Munich for a research project as shown in Fig. 26 [WAT13], [NIT05].
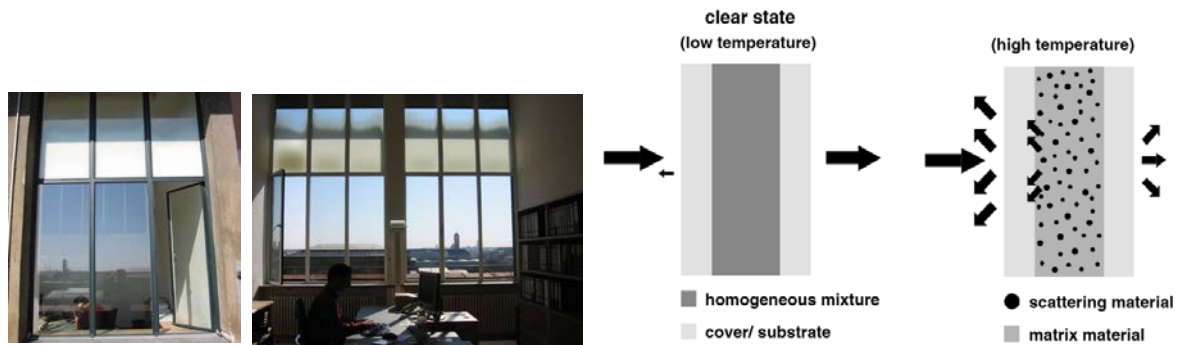
Figure 26: Thermotropic glazing, Technische Universitat München, Affinity's intelligent windows.

Developped by Okalux and the Fraunhofer institute, the thermotropic shading system T-OPAL$^{®}$ consists of a polymeric layer in the glazing elements [FRA13], [SEE10]. The method for producing this thermotropic casting resin has been patented in 2000 [BIC00].

The only commercially available thermotropic glazing to our knowledge is Solardim$^{®}$ Eco. It is made by the German company Tilse [TIL13] produces a thermotropic glazing called Solardim$^{®}$ Eco. This glazing is used in energy saving self-regulating windows [SEE12].

E.2. Characterisation of commercially available thermotropic glass

The optical properties in visible and near-infrared ranges of a commercially available thermotropic glass pane have been measured using an integrating sphere. Thus, it was possible to measure the total and diffuse transmittance and reflectance as shown in Fig. 27.
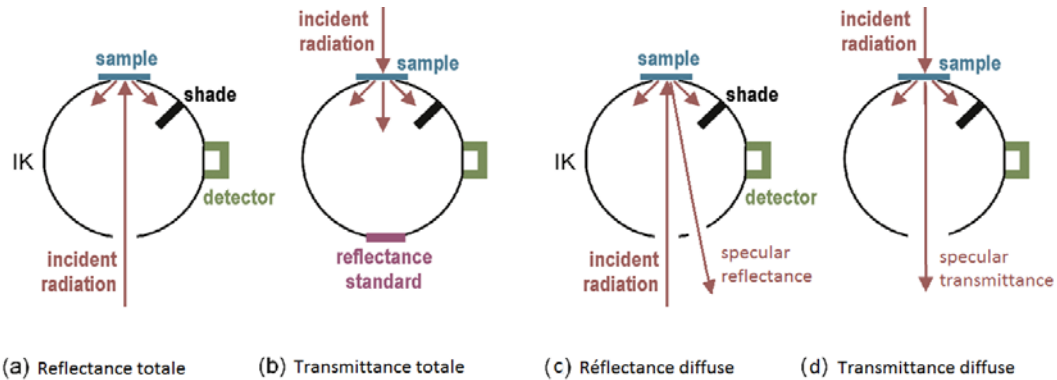
Figure 27: Principle of measurement of the total and diffuse transmittance and reflectance measurements.

The total transmittance $T(\lambda)$ and reflectance $R(\lambda)$ in the VIS-NIR range were measured for the clear and hazed states. Using this data, the total solar energy transmittance and reflectance were calculated (according to EN 410) (see Table 3).

The absorptance $A(\lambda)$ is calculated using $T(\lambda) + R(\lambda) + A(\lambda) = 100\%$.

State	Total energy transmittance	Total energy reflectance
Clear	43.47%	5.2%
Hazed	30.32%	5.9%
Difference	13.16pp	0.7pp

Table 3: Total energy transmittance and total energy reflectance for the measured thermotropic glazing.

Even in the clear state, the measured thermotropic glazing exhibits less than 50% transmitted energy. This would reduce considerably the efficiency of a solar collector and is therefore not sufficient. There is no significant change in reflection, which is around 5-6%. It is only a bit more than a single glass to air interface (~ 4%). Because reflection does not change, and transmission is reduced by only 13pp, it means that mainly the absorbance is increasing in the hazed state. **See Confidential appendix for further details.**

The product tested in this study does not offer a transition large enough to allow the use as a protection for overheating. Doping can change the properties of thermotropic glazing. Muehling et al. have investigated how the particle size can increase back scattering: "Samples containing particles of high median diameter (4800 nm) primarily scatter in the forward direction. However, with smaller particles (300 - 600 nm) a higher backscattering (reflection) efficiency was achieved." [MUE09]. Yet, the total transmittance in the clear state is still reduced and would decrease the efficiency of the collector.

Therefore, the characterized product is in its current form not suitable for our application. Thermotropic resins and the nanometric/micrometric components for thermotropic glazing have to be improved. It would be more interesting to have a layer able to reflect most of the energy.

E.3. Characterisation of a commercially available switchable mirror

In the previous part, a thermotropic glass has been studied. The product transition can be adjusted with the level of doping of the embedded resin; however it seems that it would still not be responding in a way suitable for our application. More reflection would be preferable. Following this we had the opportunity to test a switchable mirror. Although, this is an electric device and would not be a passive solution, characterisation was performed in order to evaluate the potential of this kind of product.

The switchable glass is composed of a single layer Chiral Liquid Crystal (CLC, also called Cholesteric Liquid Crystal) mixture between two Indium-Tin-Oxide (ITO) electrodes coated with a polyimide layer and two optically transparent substrates. When no current is applied, CLC forms a planar structure which naturally reflects light. The clear state occurs with all CLC helices unwounded and aligned with the electric field.

The product received at EPFL/LESO-PB effectively demonstrates quick transition. In addition, as illustrated by Fig. 28, it showed a highly reflective state and a clear transmitting state.
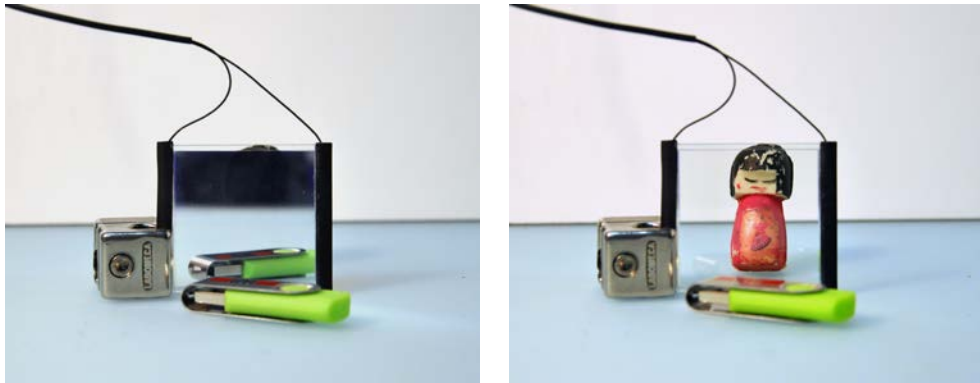
Figure 28: Switchable mirror: left, in mirror state (power OFF) and right, transparent state (power ON) (photography: Olivia Bouvard, EPFL/LESO-PB).

The direct transmittance was measured in the UV-VIS-NIR range (350-2100 nm) in the clear and the reflective state. This product exhibits high value of transmittance in the visible range in the clear state and very low transmittance in reflective state.

As presented in Table 4, the fraction of solar spectrum transmitted is 41.2%, while the part of the visible light (according to human sensibility) is only 1.4%. This switchable mirror has been designed to reflect the visible light. Visible transmittance is reduced to 1.4% in the mirror state and in the clear state transmittance is superior to 87%. **See Confidential appendix for further details.**

State	Solar transmittance	Visible transmittance
Mirror	41,2%	1,4%
Clear	82,8%	87,7%
Difference	41,6pp	86,3pp

Table 4: Solar transmittance and visible transmittance for the measured switchable mirror.

The measured switchable mirror exhibits interesting optical properties. For further improvement, the spectral properties of chiral liquid crystals can be tuned depending on the properties of the crystals.

However, when no tension is applied, the glazing stays in the mirror state. Furthermore, there is still no information on long-term longevity under heat and UV-light. If this kind of product is to be applied for solar collector, the lifetime in harsh conditions should be at least 25 years.

Evaluation

Our thermochromic solar absorber coatings are inorganic, selective, and show a perfectly reversible phase transition at a critical temperature implying a considerable change of the thermal emissivity. For the pure thermochromic material, the transition temperature of 68°C is relatively low and should be increased to approx.. 95°C. By computer simulations it could be estimated that the energy losses due to the mismatch of the transition temperature are below 14%.

Literature studies suggested that it might be possible to increase the transition temperature by doping the coatings with aluminium. In our experiments, aluminium doping has led to an amorphisation of the film structure leaving the transition temperature unchanged. On the other hand, a stronger switch in thermal emittance might be achieved by aluminium doping.

Using a novel type of doping, we showed that **it is principally possible to increase the transition temperature**. In preliminary experiments, a transition temperature of 85°C has been achieved.

Possible approaches for further optimisation might be a variation of the process parameters such as the substrate temperature, or doping by other elements.

The switch in thermal emissivity limits the temperature of the absorber to values below the temperature of degradation of glycol (160°C-170°C).

However, it would be preferable to limit the temperature to approx. 100°C, avoiding likewise the formation of the used water-glycol mixture. In order to limit the temperature of the absorber below 100°C, the primary switch in thermal emissivity might trigger a secondary switch in the solar transmittance of a thermochromic or thermotropic collector glazing.

The thermal coupling between the solar absorber sheet and the glazing of the collector has been studied by numerical computations, and the range of preferable transition temperatures has been identified. The optical properties of a commercially available thermotropic glazing have been characterized. These investigations showed that in its current form the product is not yet satisfying, and would have to be improved for the envisaged application. As an alternative, switchable mirrors have been considered. Their optical properties are more promising, but open questions remain concerning e.g. cost and durability. Our thermochromic coatings could also be used on the collector glazing, and are therefore a promising alternative.

Within this project, significant progress has been made in the field of thermochromic solar collectors. The scientific findings open up fascinating new perspectives for the future of smart materials for solar thermal collectors.

Acknowledgements

Industry Contacts

- Interaction and discussions with ALCAN that shows a general interest in our research development
- CTI project on sol-gel deposition of nanostructured selective solar absorber coatings in collaboration with the Swiss solar collector manufacturer ENERGIE SOLAIRE SA
- ASULAB (SWATCH GROUP) donated equipment for vacuum deposition of thin films, suitable for multilayer deposition
- Partnership with SWISSINSO: technology transfer of magnetron sputtering and research on novel coatings for innovative solar collector glazing

National scientific collaborations

- Active participation of Dr. Rosendo Sanjines and Henry Jotterand, Laboratory of Thin Films Physics, Prof. Laszlo Forro, Institute of Complex Matter Physics, EPFL. Experiments on magnetron sputtering and X-ray diffraction analysis

- Within EPFL, access to electron microscopes and to the facilities of TEM sample preparation is provided by the Interdepartmental Center of Electron Microscopy CIME.

- The research group of Prof. Libero Zuppiroli (LOMM at EPFL) provides access to their new ellipsometer. This contact will be useful for future measurements of the optical properties of thermochromic coatings.

- Collaboration with the research group of Prof. Peter Oelhafen, Institute of Physics, University of Basel.

- The research group of Prof. S. Mikhailov (IMA-Arc) provided access to their Van der Graaff accelerator for the RBS analyses.

- The research group of Prof. F. Bussy at UNIL in the Mineralogy and Geochemical Institute provided access to their EPMA JEOL 8200 super probe equipment for WDS analyses.

International scientific collaborations

- An informal scientific collaboration exists with the Polymer Competence Center Leoben (PCCL) in Austria.

- Informal scientific collaboration with the Department for Energy at Politecnico di Torino with Prof. M. Perino and Prof. V. Serra and Dr. L. Bianco.

Invited Presentations

A. Krammer, *Effect of doping on VO$_2$ thermochromic thin films deposited by magnetron sputtering, Master defence*, September 1st, 2014, Grenoble INP, France.

A. Schüler, *Neues von der Glasfront*, invited plenary talk, September 26th, 2014, conference EcoBau1014, Bern, Switzerland

A. Schüler, *Innovative Coloured Solar Glass for Enhanced Building Integration of Solar Energy Systems, conference EcOrient 2014*, June 4th, 2014, Beirut, Lebanon

A. Schüler, *Nanocomposite optical coatings for solar energy conversion,* Basler Forschungs Forum, BASF Switzerland, March 26th, 2014, Basel, Switzerland

A. Schüler, *Nanocomposite optical coatings for solar energy conversion,* November 26th, 2013, Department of Energy, Politecnico di Torino, Italy

A. Schüler, *Couches minces optiques composées de matériaux nanocomposites pour applications dans le domaine de l'énergie solaire*, colloque: "Nanotechnologies: une autre vision sur les énergies", entretiens Jacques Cartier, November 19th, 2012,INSA de Lyon, France

Publications

A. Paone, PhD thesis, **Switchable selective absorber coatings for overheating protection of solar thermal collectors**, EPFL thesis No. 5878, Lausanne, Switzerland, 2013

A. Paone, R. Sanjines, P. Jeanneret, H. J. Whitlow, E. Guibert, G. Guibert, F. Bussy, J.-L. Scartezzini, and A. Schüler. **Influence of doping in thermochromic V$_{1-x}$W$_x$O$_2$ and V$_{1-x}$Al$_x$O$_2$ thin films: twice improved doping efficiency in V$_{1-x}$W$_x$O$_2$**. Accepted in the Journal of Alloys and Compounds, 2014.

A. Paone, R. Sanjines, P. Jeanneret, and A. Schüler. **Temperature-dependent multiangle FTIR-NIR-VIS-UV ellipsometry of thermochromic VO$_2$ and V$_{1-x}$W$_x$O$_2$ films**. Submitted to Solar Energy Materials and Solar Cells, 2014.

A. Paone, M. Geiger, R. Sanjines, and A. Schüler. **Thermal solar collector with VO$_2$ absorber coating and V$_{1-x}$W$_x$O$_2$ thermochromic glazing - temperature matching and triggering**. Accepted in Solar Energy, 2014.

Conferences

W. A. Vitale, A. Paone, M. Fernández-Bolaños, A. Bazigos, W. Grabinski, A. Schüler, and A. M. Ionescu. **Steep slope VO$_2$ switches for wide-band (DC-40 GHz) reconfigurable electronics**. In Device Research Conference, Santa Barbara (California), 2014.

W. A. Vitale, A. Paone, C. F. Moldovan, A. Schüler, and A. M. Ionescu. **Growth optimization of vanadium dioxide films on SiO$_2$/Si substrates**. In Micro and Nano Engineering Conference, Lausanne (Switzerland), 2014.

References

[And54]   G. Andersson. **Studies on Vanadium Oxides**, Acta Chemica Scandinavica, 8:1599-1606, 1954.

[Bal08]   A. Baldi, D. M. Borsa, H. Schreuders, J. H. Rector, T. Atmakidis, M. Bakker, H. A. Zondag, W. G. J. van Vanhelden, B. Dam, and R. Griessen. **Mg-Ti-H thin films as switchable solar absorbers**, International Journal of Hydrogen Energy, 33(12):3188{3192, June 2008.

[Cul78]   B. D. Cullity. **Elements of X-ray diffraction**, Addison-Wesley Publishing Company Inc., 2nd edition, 1978.

[Fai91]   Prof. A. Faist, **Physique du bâtiment I et II**, 1991.

[Goo71]   J. B. Goodenough. **The Two Components of the Crystallographic Transition in VO$_2$**, Journal of Solid State Chemistry, 3:490 - 500, 1971.

[Huo08]   G. Huot, C. Roecker, Dr. A. Schüler, *Evaluation of the Potential of Optical Switching Materials for Overheating Protection of Thermal Solar Collectors*, SFOE project #102016 (2008).

[Pao09]   A. Paone, M. Joly, R. Sanjines, A. Romanyuk, J.-L. Scartezzini, A. Schüler, *Thermochromic films of VO$_2$:W for "smart" solar energy applications*, Proc. SPIE 7410, 74100F (2009)

[Sol06]   M. Soltani, M. Chaker, E. Haddad, R. V. Kruzelesky. **Thermochromic vanadium dioxide smart coatings grown on Kapton substrates by reactive pulsed laser deposition**, Journal of Vacuum Science & Technology A: Vacuum, Surfaces, and Films 24 (3) (2006) 612.

[Vries98]   D. de Vries. **Design of a photovoltaic/thermal combi-panel**, PhD thesis, Technical University of Eindhoven, 1998.

[Zon03]   H. A. Zondag, D. W. de Vries, W. G. J. van Helden, R. J. C. van Zolingen and A. A. van Steenhoven. **The yield of different combined PV-thermal collector designs**, Solar Energy, 74(3):253{269, March 2003.

[IDW]   Frank P. Incropera, David P. DeWitt, **Fundamentals of Heat and Mass Transfer**.

[NAV13]   Matthew Ulterino, Eric Bloom, **Smart glass**, Navigant Research, 3Q 2013

[NIT05]   Nitz, P., Hartwig, H., 2005**. Solar control with thermotropic layers**. Solar Energy 79, 573–582.

[WAT13]   Watanabe, H. **watanabe@afty.jp**. RE: EPFL thermotropic windows. 08 Aug 2013.

[FRA13]   **Thermotropic sunshading system** - Fraunhofer IBP, n.d. URL
              http://www.ibp.fraunhofer.de/en/Product_Development/Thermotropic_sunshadingsyste

m.html

[SEE10]   Seeboth, A., Ruhmann, R., Mühling, O., 2010. **Thermotropic and Thermochromic Polymer Based Materials for Adaptive Solar Control**. Materials 3, 5143–5168.

[BIC00]   Bicer, T.; Schwitalla, C.; Gödecke, H. **Method for Producing Thermotropic Casting Resin Systems**. DE Patent 19825984, 16 March 2000.

[TIL13]   **Solardim Eco** : self-regulating solar reflecting windows. For both plane and bent compound glazing, n.d. URL http://www.tilse.com/tilse/en/glas/solardim-eco.php

[SEE12]   Seeboth, A., Fraunhofer-Institut für Angewandte Polymerforschung IAP, SOLARDIM®-ECO **High energy savings through self-regulating solar protection glazing**. 2012. http://www.iap.fraunhofer.de/content/dam/iap/en/documents/FB2/Solardim_ECO_Seeboth_EN_2012.pdf

[MUE09]   Muehling, O. et al. **Variable solar control using thermotropic core/shell particles**. Solar Energy Materials and Solar Cells 93, 1510–1517 (2009).